JOURNAL OF CHEMICAL & ENGINEERING DATA

ARTICLE

pubs.acs.org/jced

Methodology for the Development of Thermodynamic Models Describing Substances That Exhibit Complex Association Interactions

Barath Baburao* and Donald P. Visco, Jr.

Department of Chemical Engineering, Tennessee Technological University, Box 5013 Cookeville Tennessee 38505, United States

ABSTRACT: This work describes a methodology for the development of a thermodynamic model describing the substances that show strong self- and cross-association interactions. The methodology is fundamentally based on the chemical theory of association interactions. The system used as a case study in this work is a binary mixture containing hydrogen fluoride and water (HF + H_2O). Earlier studies have failed to provide a reasonable description of this binary mixture because of the complex association interactions between these compounds, which were not adequately modeled. In this work, the phase behavior of this mixture is understood by exploring these complex association interactions. Pure HF was modeled using 14 different association schemes that allow the formations of different physically meaningful oligomers with different distribution schemes (1−2, 1−6, 1−2−6, etc.), where the 1−2 scheme allows the formation of monomers and dimers and likewise. The parameters for these pure component schemes were obtained by correlating the phase coexistence properties of pure HF and were also used to predict several other pure component properties (ΔH_{vap}, C_P, C_v, Z, etc.) The dominance of these association patterns and their distribution were understood on the basis of their predictive ability. The pure component association schemes that were developed for HF and water were extended to the binary mixture. The phase coexistence properties were correlated using different association patterns for the pure components with and without considerations for the strong association between them. The significance of these self- and cross-association patterns are studied and understood on the basis of the correlative and the predictive ability of the association schemes. The effect of including the cross-associates that are most likely to be formed in this mixture, from a molecular level hybrid meta-density functional theory study, is also discussed. The methodology described in this work can be utilized to understand and predict the bulk-phase thermodynamic properties of substances that show complex association interactions at a molecular level.

INTRODUCTION

In the chemical process industry, accurate knowledge of thermophysical properties of various substances is essential in both process as well as product development stages of operation. The cost involved in experimental measurements of these thermophysical properties and also the imposed time-constraints emphasize the necessity for robust and predictive thermodynamic models.[1] On the other hand, the development of robust and highly predictive thermodynamic models is not a simple or straightforward exercise. This is especially true for substances that exhibit complex molecular level interactions, especially when using traditional or even more current thermodynamic modeling techniques. The predictive ability of these thermodynamic models is dependent on their accuracy in incorporating the intra- and intermolecular forces that play a vital role in the macroscopic behavior of the system. Hence, a key factor is to understand the molecular level interactions and account for them in a model that can predict bulk-phase properties.

In this work, we propose a methodology for modeling substances that show complex molecular level association interactions. The methodology described in this work can be utilized to understand and predict the bulk-phase thermodynamic properties of substances that show complex association interactions at a molecular level. This methodology is fundamentally based on the work discussed decades ago by Heidemann and Prausnitz[2] on the chemical theory of association interactions. Ever since this work was reported, incorporating association into cubic equations of state has been in practice for correlating and predicting the phase coexistence properties. In this approach, it is necessary to know the types of oligomer species that are present in the system. The formation of these oligomers is described as a series of chemical reactions with appropriate equilibrium constants. A cubic equation of state is then included to describe the physical interactions between the associated species. This approach provides the freedom to specify the existence of the oligomers beforehand, if such information is available. The exercise of obtaining this important information on the distribution of oligomers in a nonideal environment is a challenging endeavor. With computational chemistry techniques, however, this can be identified with a reasonable level of accuracy.

For some associating substances, there can be several types of oligomers that are present at the molecular level in the form of monomers, dimers, trimers etc., but the distribution need not be the same. In this work, we discuss the impact on the correlation and prediction of bulk-phase thermodynamic properties by using a methodology which allows including both the type and distribution of oligomers.

The system used as a case study in this work is a binary mixture containing hydrogen fluoride and water (HF + H_2O). This particular binary mixture serves as a very good model for substances that are difficult to work with experimentally due to its

Special Issue: John M. Prausnitz Festschrift

Received: November 8, 2010
Accepted: February 12, 2011
Published: March 14, 2011

ACS Publications © 2011 American Chemical Society

corrosive nature and also as one that exhibits complex association interactions at the molecular level.

Modeling hydrogen fluoride (HF) is difficult in its own right; adding a highly polar and associating compound like water only increases its complexity. Unlike water, which associates in the liquid phase and shows limited association in the vapor phase (the compressibility factor of water vapor at 1 atm is 0.98),[3] HF associates in both liquid and vapor phases (the compressibility factor of HF vapor at 1 atm is 0.29).[4] These associating, pure components, when in mixtures, potentially can form a variety of cross-associates. This association affects the properties of aqueous mixtures of HF, resulting in a highly nonideal behavior that does not lend itself to traditional modeling techniques. The conjecture, then, is that to develop an accurate, bulk-phase thermodynamic model describing the properties of complex associating mixtures with two components that can hydrogen bond (such as aqueous HF), one has to properly account for the association schemes both in the pure components and in the mixtures. These association patterns in the aqueous HF system are yet to be determined experimentally. There are very few theoretical studies[5−8] that have attempted to answer the structural properties of this mixture. There has been only one attempt to model this mixture in the bulk phase, and this study was reported to agree with the available experimental vapor pressure results, but fails in predicting the heat effects that are essential during the modeling of separation stages of the process.[9] The unique and challenging associating nature of the mixture combined with the modeling shortcomings as well as its major industrial importance establishes the complexities and the need for the development of a robust and predictive thermodynamic model. As mentioned earlier, the methodology that is used in this work can also be used to thermodynamically describe any other strongly associating mixtures with such substances as HCl and H_2SO_4.

The paper is ordered as follows. First we describe the methodology used to model multicomponent mixtures (binary in this case study) showing strong association interaction. Then we discuss the basic equations for the formulation of the pure component bulk-phase thermodynamic model. We then discuss the correlated and predicted results for pure water and HF using various association schemes. We then describe the extension of these association patterns into a binary mixture with and without considerations for association interactions between HF and water. We also describe the theoretical study that was performed to understand the distribution of cross-association patterns at the molecular level via a computational chemistry approach. After this we discuss the correlative and predictive results for the mixture using different association schemes. Finally, we will draw conclusions based on the results that are reported in this work.

Description of Methodology. It is thought that a detailed accounting of the self-and cross-association interactions in strongly associating mixtures where both components can hydrogen bond will lead to a robust and predictive thermodynamic model. To describe and evaluate the methodology, the model mixture that was chosen to work with as a test case is the aqueous hydrogen fluoride system. This section describes the plan that was adopted in the development of the thermodynamic model of this system. The flow sheet (Figure 1) illustrates the plan in detail.

Since the primary objective here is to explore the effect of association schemes on modeling substances that shows strong association interactions, a reasonable place to start is with the simplest association scheme possible and then add degrees of complex interactions. In phase 1 of Figure 1, a systematic approach was used in modifying the association scheme to develop correlative and predictive pure component models. Such an approach is inherently iterative in the sense that a good model for VLE will then be assessed against other (industrially important) experimental data that were not used during the model parametrization (such as enthalpy, heat capacity). If, for example, the model is not predictive of this property, then this additional data will be used during parametrization. If the simplistic model fails to be predictive after all iterations, the association scheme is modified and the parametrization process is started for the new association scheme. In the case of multicomponent mixtures, this should be performed for all the substances in the mixture before implementing the association scheme in the mixture stage.

We start phase 1 with reasonable upper-limit values on the number of oligomers that can be formed. For the case of pure HF, the upper limit on the oligomer size was set at 12, which is reasonable in light of other association schemes previously used to describe HF vapor.[10] Both levels of iteration (to include more experimental data during correlation and in modifying the association schemes) are shown as dashed lines in Figure 1. Once optimal pure component models for both HF and water have been found in this manner, the models serve as the input for phase 2.

Once the association schemes for the pure components are obtained (pure HF and H_2O in this case) from phase 1, those models will be used in the binary mixture. Accordingly, it is necessary to explore the association patterns in the mixture. Molecular level studies and pre-existing spectroscopic information[5,7,11] can be used in this phase to aid in the choice of the various association patterns possible in this mixture. In this case study, most of the existing molecular level studies on the HF + H_2O mixture have been directed toward issues such as the proton transfer complex and vibrational properties.[5−8] Therefore, computational chemistry studies were conducted specifically toward gaining information on association patterns in this mixture using energy considerations to eliminate poor-performing cross- and self-associates. Note that this step is specifically designed as a coarse-grained or filtering step since the number of possible cross-associates that can actually be formed (depending on the pure component model) may be very large. Once the preferred clusters in the mixture are identified, the bulk-phase model for mixtures will include these clusters during the correlation and prediction stage of the model development.

Once again, the poorly predicted property (if any) will be included in the correlation cycle with changes in the association schemes of the mixture, say by including cross-association and/or by choosing different cross-association patterns, through the iterative procedure indicated by dashed lines in phase 2. Once the potential combinations (short listed from molecular level studies) of cross-association schemes in the mixture are used, an option exists to go back to the pure component association schemes and generate new pure component models. This step is required since multiple pure component models (re: association schemes) may perform similarly during phase 1 but could have drastically different performances during phase 2. In theory, the final robust model will be correlative with respect to the available literature or new generated experimental data and it will also be predictive so that it can be used to determine all the available properties of this mixture at any feasible conditions of temperature and pressure. The next section will describe in detail the pure component association models for the case study here, HF and water.

Pure Component Association Model. Molecules with dipole moments attract each other electrostatically by lining up with

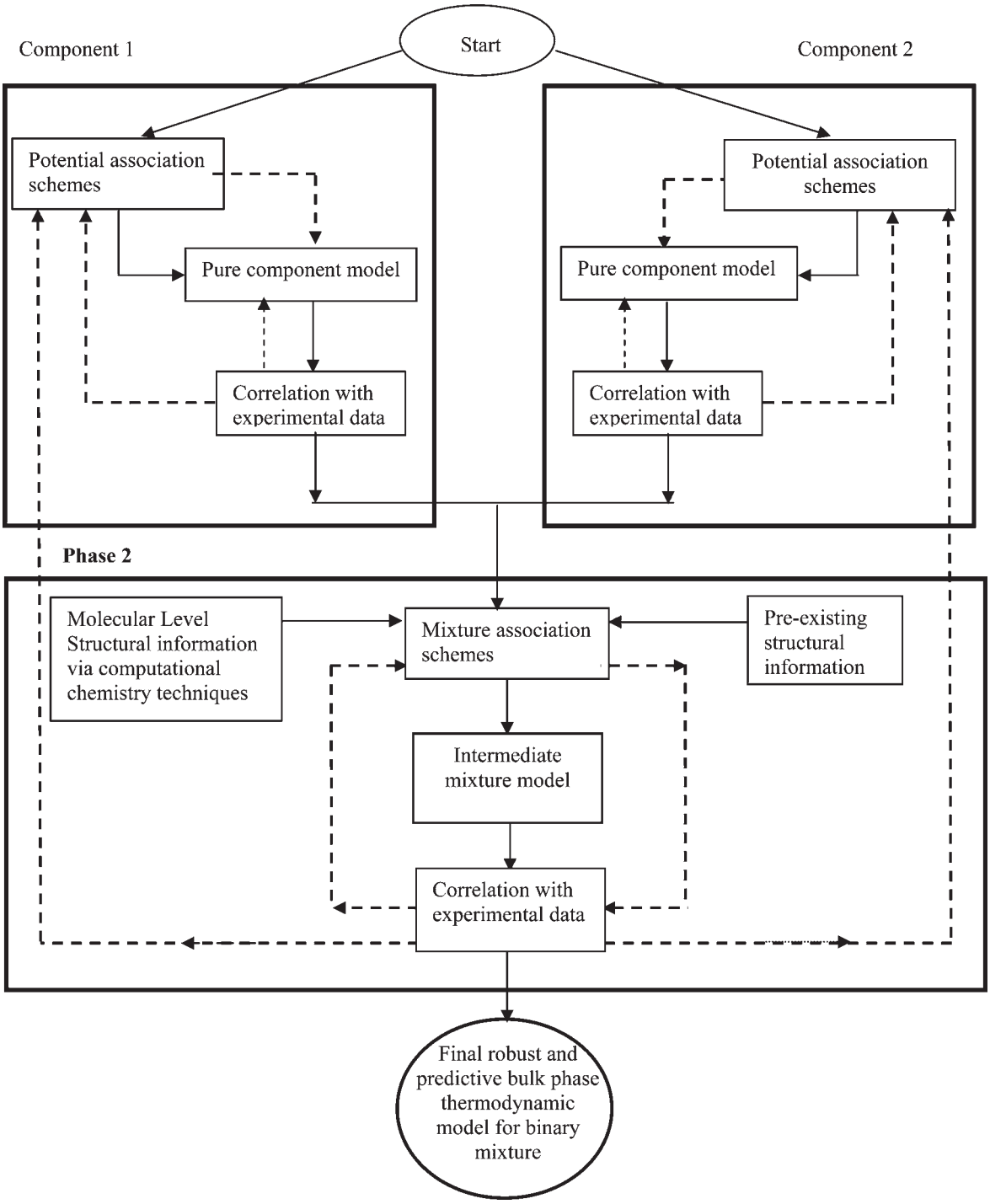

Figure 1. Methodology for the development of a robust and predictive bulk-phase thermodynamic model for strongly associating mixtures.

their oppositely charged ends. These dipole−dipole forces are particularly strong among the molecules in which the hydrogen atom is attached directly to a highly electronegative atom such as fluorine, oxygen, nitrogen etc. Both HF (μ_{HF} = 1.83 D[12]) and H_2O (μ_{H_2O} = 1.85 D[13]) are polar substances of this type, and henceforth show strong H-bonding interactions. These association interactions are extremely important and have a significant effect on microscopic as well as macroscopic properties. In the case of water, if H-bond interactions were not present, the estimated melting point of ice is 183 K and the boiling point of water would be 193 K.[14,15] On the other hand, several anomalies in HF, including a predicted isothermal compressibility peak,[16] have been attributed to its vapor-phase association. Accordingly, when these association interactions have such a profound effect on the thermodynamic properties of interest, it is imperative to include these interactions accurately while developing a predictive bulk-phase model.

Since HF and water show distinct, multidimensional H-bond networks,[17] a model that allows the formation of specific oligomers for both pure components will be useful to test the

correlative and predictive ability of several kinds of association patterns. There are several models describing the thermodynamic properties of HF through assumption of various association schemes.[4,10,17−23,25] Anderko and co-workers developed a thermodynamic model (herein after called the AEOS model) for pure HF and its mixtures[25] using chemical association theory. Prausnitz and his co-workers explored this kind of an association-based equation of state for substances like water, acetonitrile, and argon in the late 1970s.[2,24] In this model, the phase coexistence properties of the substances showing strong association are determined by treating association interactions separately as a series of chemical reactions, and subsequently including the physical interactions between these otherwise ideal clusters via a conventional cubic equation of state. These two contributions are included by separating them in terms of compressibility factor (Z). Henceforth, the model is best described in terms as $Z = Z^{ch} + Z^{ph} - 1$. The chemical part, Z^{ch}, describes the formation of clusters (oligomers) from single monomeric units through appropriate association schemes, while the nonspecific interactions between these oligomers are described by the physical part (Z^{ph}).

In the AEOS model for HF, to account for the propensity of a system to form specific oligomers at the expense of others, a Poisson-like distribution as a function of chain length is used.[25] This kind of association scheme, which is continuous, allowed for the formation of any oligomers, yet is constrained toward the formation of particular *i*-mer, proved to be successful in correlating and predicting the phase coexistence properties of pure HF as well as some binary mixtures.[25,21,26] However, such an approach only used limited cluster evidence in model development. In this work, 14 different association schemes are evaluated for their correlative and predictive ability in order to illustrate the importance of the inclusion of accurate association patterns for substances that shows strong H-bond interactions.

Formulation of the Model. First we shall introduce the Z^{ch} formulation for each association scheme. On the basis of the ideal association solution model introduced by Wooley[27] and corroborated by Heidemann and Prausnitz,[2] Z^{ch} can be expressed as a ratio of the actual number of moles of all species in the associated mixture (n_T) to the number of moles at the absence of association (n_0).[25] This ratio can be calculated by considering the equilibrium constant of the consecutive association reaction,

$$jA_1 \rightarrow A_j \tag{1}$$

where A is any associating compound, the subscript indicates the corresponding j-mer. The equilibrium constant for the above reaction is specified by[28]

$$K_j = \frac{z_{A_j}}{z_{A_1}{}^j} \frac{1}{(P^{ch})^{j-1}} \tag{2}$$

where z_{A_j} is the respective oligomer mole fraction for the j-mer and $P^{ch} = RTZ^{ch}/v$, is the total pressure due to the chemical part, with R the universal gas constant, T the temperature, and v the specific volume. The chemical contribution, $Z^{ch} = n_t/n_0$, can now be expressed as

$$Z^{ch} = \frac{\sum_{j=1}^{N} K_j \left[\frac{RTZ^{ch}}{v} z_{A_1}\right]^j}{\sum_{j=1}^{N} jK_j \left[\frac{RTZ^{ch}}{v} z_{A_1}\right]^j} \tag{3}$$

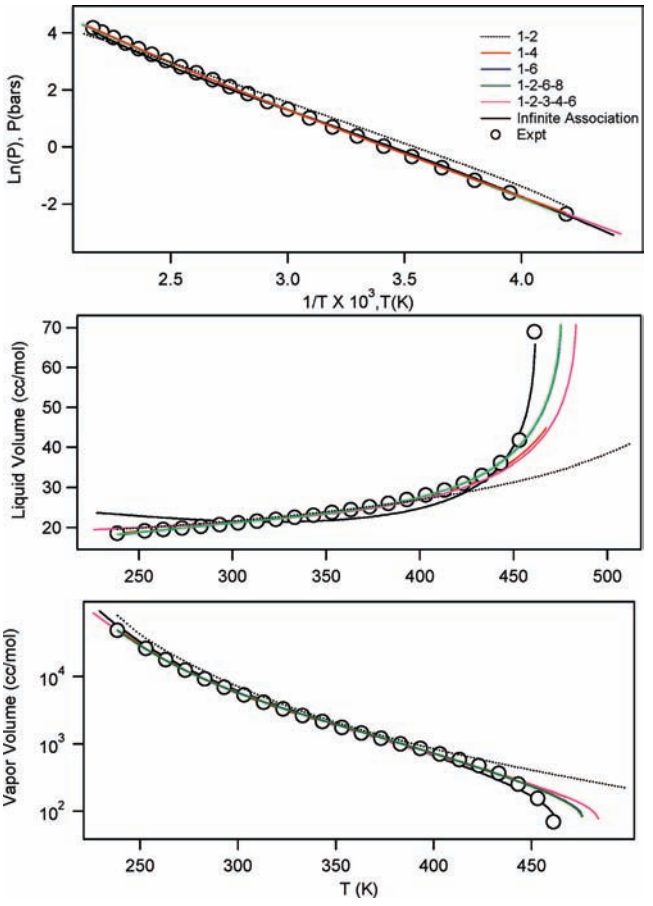

Figure 2. Pure HF VLE from different association models compared with experiment.[4]

In eq 3, N is the maximum number of oligomers that are allowed to form on the basis of the association scheme adopted. Note that that the chosen association pattern is not always consecutive. For instance, one can also specify the association pattern in such a way that only monomers, dimers, and octamers are the only oligomers allowed to be formed.

On the basis of a material balance, it can be shown that

$$\frac{RT}{v} = \sum_{j=1}^{N} jK_j[\mathrm{Px}_{A_1}]^j \tag{4}$$

where

$$\mathrm{Px}_{A_1} = \left[\frac{RTZ^{ch}}{v} z_{A_1}\right] \tag{5}$$

So, to obtain a closed form expression for Z^{ch}, one needs to solve for Px_{A_1} in eq 4 and substitute back into eq 3. It is possible to obtain a closed form analytical expression for Z^{ch} for only a few association schemes;[29] for the rest Z^{ch} has to be solved numerically.

In the AEOS model, the equilibrium constant of these association reactions are expressed as a product of a weighting function and the dimerization constant, K. As suggested earlier, a Poisson-like distribution was used to include specific oligomers at the expense of less important ones. In the current work, we replace this Poisson-like distribution function by a free

Table 1. Parameter Values and % AAD Values for Pure HF Association Schemes

parameter	1−2	1−4	1−6	1−2−3	1−2−6	1−3−6	1−2−12
f_1	0.8570	1.5090	1.0407	1.4618	1.0426	1.0477	0.5801
f_2	2.0508	0.1264	0.1607	0.6532	0.1654	0.1659	0.1591
f_3	0.0230	−1.5254	−0.8321	−0.0689	−0.8420	−0.8530	−0.7863
B (cc/mol)	15.2051	12.2079	10.7077	13.4072	10.7263	10.7549	8.4514
ΔH^0 (J/mol)	−38820.2911	−51770.4385	−34248.1316	−54141.9782	−34357.4269	−34155.3733	−29110.0565
ΔC_P° (J/(mol K))	20.0193	128.1303	35.6614	56.8601	33.4423	30.1542	13.9689
ΔS^0 (J/(mol K))	−105.0497	−169.5243	−129.7445	−160.9736	−134.1529	−127.7844	−102.5819
$\beta(3)$	N/A	N/A	N/A	8.3842	N/A	3.8068	N/A
$\beta(4)$	N/A	24.1494	N/A	N/A	N/A	N/A	N/A
$\beta(5)$	N/A	N/A	N/A	N/A	N/A	N/A	N/A
$\beta(6)$	N/A	N/A	2.9603×10^4	N/A	4.7927×10^5	1.4515×10^4	N/A
$\beta(7)$	N/A	N/A	N/A	N/A	N/A	N/A	N/A
$\beta(8)$	N/A	N/A	N/A	N/A	N/A	N/A	N/A
$\beta(9)$	N/A	N/A	N/A	N/A	N/A	N/A	N/A
$\beta(10)$	N/A	N/A	N/A	N/A	N/A	N/A	N/A
$\beta(11)$	N/A	N/A	N/A	N/A	N/A	N/A	N/A
$\beta(12)$	N/A	N/A	N/A	N/A	N/A	N/A	4296.8884
% AAD − P	25.5231	**1.1370**	**1.6783**	17.2307	**1.1803**	**1.1853**	2.8792
% AAD − v^{liq}	4.9324	**1.7763**	**0.7130**	3.8169	**0.7009**	**0.7148**	2.5908
% AAD − v^{vap}	32.3550	**4.6844**	**4.8050**	34.0684	**4.7880**	**4.6385**	5.5852

parameter	1−2−6−8	1−2−3−4−5	1−2−3−4−6	1−2−3−6−9	1→9	1→12	∞
f_1	0.8450	0.1165	0.0830	0.7525	0.8609	0.8078	0.0826
f_2	0.1898	1.5058	1.5794	0.1879	0.2023	0.2180	0.7554
f_3	−0.7573	−0.0494	−0.0925	−0.7612	−0.7401	−0.6262	−0.2510
B (cc/mol)	9.9818	12.1713	12.2247	9.5245	10.1119	9.9581	8.9588
ΔH^0 (J/mol)	−31625.2748	−54952.5784	−61923.3349	−30948.9598	−32040.8098	−32335.2096	−30134.5155
ΔC_P° (J/(mol K))	21.9344	182.8244	236.1244	22.9567	24.6708	36.1455	62.1233
ΔS^0 (J/(mol K))	−122.1599	−175.8064	−198.8777	−119.0219	−124.3294	−125.9036	−98.7913
$\beta(3)$	N/A	1.0005	2.2238	5.1622	2.2420	1.6038	N/A
$\beta(4)$	N/A	12.5749	18.7302	N/A	14.0734	15.8340	N/A
$\beta(5)$	N/A	1.2997	1.2751	N/A	404.8991	644.6536	N/A
$\beta(6)$	1.4749×10^4	N/A	N/A	4012.6854	1.3538×10^4	9.3660×10^3	N/A
$\beta(7)$	N/A	N/A	N/A	N/A	2.9390×10^5	2.1771×10^5	N/A
$\beta(8)$	N/A	N/A	N/A	N/A	1.4875×10^6	2.7801×10^5	N/A
$\beta(9)$	N/A	N/A	N/A	5.5220×10^6	2.5221×10^6	5.4463×10^6	N/A
$\beta(10)$	N/A	N/A	N/A	N/A	N/A	4.1884×10^6	N/A
$\beta(11)$	N/A	N/A	N/A	N/A	N/A	1.2073×10^7	N/A
$\beta(12)$	N/A	N/A	N/A	N/A	N/A	9.3588×10^6	N/A
% AAD − P	**2.011**	5.0515	2.4564	2.5322	2.1275	2.7242	8.5092
AAD − v^{liq}	**1.001**	1.2952	2.9498	1.3886	0.9813	0.9647	8.5993
% AAD − v^{vap}	**4.8646**	11.0181	6.2506	4.9831	4.9111	5.1240	7.9646

parameter that is modified on the basis of the association pattern used. Therefore,

$$K_j = \beta(j)K^{j-1} \tag{6}$$

where $\beta(j)$ is the parameter for the corresponding j-mer. For a monomer, $K_1 = 1$ and $\beta(1) = 1$, and for a dimer, $\beta(2) = 1$. The temperature dependent dimerization constant, K, is expressed as

$$\ln K = \frac{-\Delta H^0 + \Delta C_P^0 T^0}{RT} + \frac{1}{R}(\Delta S^0 - \Delta C_P^0(1 + \ln T)) + \frac{\Delta C_P^0 \ln T}{R} \tag{7}$$

where ΔH^0, ΔS^0, and ΔC_P^0 are the standard enthalpy, entropy, and heat capacity of association, respectively, with the superscript "0" corresponding to the reference state temperature of 273.15 K.

The physical interaction between the aggregates are described by means of a cubic equation of state, here the Peng−Robinson equation of state (PREOS),[30] with a constant excluded volume parameter b, and a temperature dependent energy parameter $A(T)$. The energy parameter $A(T)$ for HF is described as

$$A(T) = 10^6\left(f_1 + f_2 \exp\left[f_3\left(\frac{T}{100} - 4.02\right)^2\right]\right) \tag{8}$$

dx.doi.org/10.1021/je1011955 |J. Chem. Eng. Data 2011, 56, 1506–1525

where f_1, f_2, and f_3 are fitted parameters. For water, the energy parameter is characterized by three parameters, the apparent critical temperature T'_C, critical pressure P'_C, and acentric factor ω', as in the original PREOS.

In total there are four parameters for the physical part and three parameters for the chemical part that are used to fit during the correlation stage of model development. For association schemes with no analytical formulation, the number of parameters will increase on the basis of the scheme adopted. For instance, a model that allows the formation of only monomers, dimers, and hexamers (1−2−6) will have 1 additional parameter, $\beta(6)$, that will be included in the Z^{ch} during the correlation stage of modeling. These parameters are fitted to the respective pure component vapor pressure, and saturated liquid and vapor volume data. For the rest of the paper, the association schemes are named according to the oligomers that are allowed to be formed. For instance, a scheme that allows the formation of only monomers, dimers, and hexamers is called the 1−2−6 scheme. The association schemes that allow the formation of all oligomers between 1 and 9 and 1 and 12 are called 1→ 9 and 1→ 12 scheme, respectively.

PURE COMPONENT MODEL RESULTS

Pure HF. For pure HF, 14 different association schemes were evaluated. The parameters of these models are fitted to pure component vapor pressure and saturated liquid and vapor volume data.[4] Figure 2 shows the saturated vapor pressure and liquid and vapor volumes fit using 6 of the 14 different association schemes. While the parametrization is completed for all the 14 association schemes, only 6 of them are shown here for clarity. However, the parameter values and the percentage absolute average deviation (% AAD$^+$) values (for correlated properties) for all 14 different models are listed in Table 1. As can be seen, all 6 association schemes show very good agreement with the experimental data, with some inconsistencies near the critical region, especially the 1−2−3−4−6 and 1−2 schemes. Here, the infinite association model is different from what was used in the AEOS approaches.[25,21] Even though the infinite association scheme adopted here is continuous,[31] unlike the earlier approaches[25,21] for HF, it is not constrained toward the formation of a particular *i*-mer. In this association scheme, every oligomer such as monomers, dimers, trimers, etc. are allowed to form with the same frequency as others. In other words, at a given state, the number of monomers allowed to be formed by this model will be the same as dimers, trimers, tetramers, and so on. Based on the % AAD values, the 1−4, 1−6, 1−2−6, 1−3−6, and 1−2−6−8 (shown in bold face in Table 1) were the association schemes with the best correlative ability.

As suggested earlier, spectroscopy studies[32] indicate the dominance of cyclic hexamers and tetramers in HF. As one can see, the association schemes with hexamers are reported to possess high correlative ability as opposed to the schemes without them. The correlative ability of the association schemes that allow only one oligomer other than the monomer (1−2, 1−4, 1−6) were improved by a large extent when the dimer was replaced by a tetramer or a hexamer, corroborating the importance of hexamers[32,33] and tetramers[34] in HF. Also, the constrained association schemes that allow the formation of particular oligomers were reported with better correlative ability when compared to the unconstrained schemes, which allows any number of oligomers (infinite), or even the ones that allow the formation of higher order oligomers up to 9 and 12.

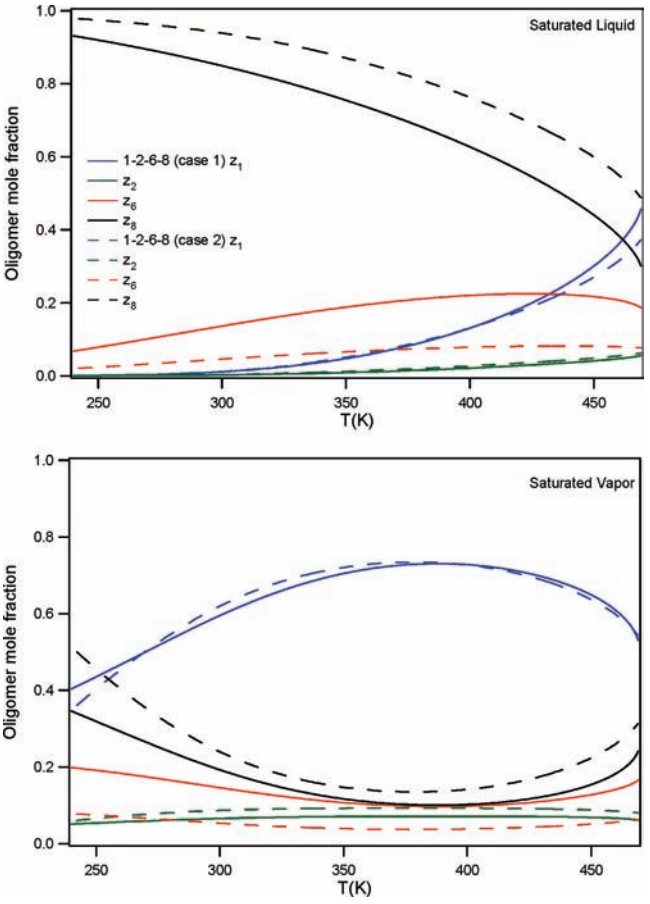

Figure 3. Distribution of oligomers across the pure HF saturation curve from two different 1−2−6−8 schemes. Here z_i indicates the mole fraction of the corresponding *i*-mer.

This indicates the significance of acquiring an accurate distribution of oligomers in HF. In pure HF, to gain high correlative ability in the bulk phase, it is essential to describe the both the association scheme and the distribution of these oligomers accurately.

Also, the optimization algorithm used (simplex method[35]) for the pure component parameter set for minimum deviations from the experimental data does not guarantee globally optimized parameters. This means for any association scheme there could be more than one parameter set that would report similar objective function values relative to the experimental data. To explore this issue on the parameter space, more than one parameter set was identified for several association schemes.

Figure 3 illustrates the oligomer distribution along the saturation curves for two different parameter sets that were obtained for the 1−2−6−8 association scheme. The parameter set for these two association schemes are listed in Table 2. As one can see, the parameter space is different from one another, with almost similar % AAD values. The distribution of the oligomers is different in both these parameter sets, which is shown in Figure 3. The relative abundance of the oligomers, especially hexamers and octamers, are different from each other in both cases. As mentioned previously, in this methodology the utility of the association scheme is evaluated by its predictive behavior. The predictive behavior for both of these models is discussed in a later section.

Table 2. Two Different Parameter Sets for 1−2−6−8 Scheme

parameter	1−2−6−8 (case 1)	1−2−6−8 (case 2)
f_1	0.8450	1.0442
f_2	0.1898	0.1652
f_3	−0.7573	−0.8328
B (cc/mol)	9.9818	10.7451
ΔH^0 (J/mol)	−31625.2748	−34273.1101
ΔC_P° (J/(mol K))	21.9344	34.7145
ΔS^0 (J/(mol K))	−122.1599	−136.1772
$\beta(3)$	0	0
$\beta(4)$	0	0
$\beta(5)$	0	0
$\beta(6)$	1.4749×10^4	1.7194×10^6
$\beta(7)$	0	0
$\beta(8)$	1.5865×10^6	4.7314×10^4
$\beta(9)$	N/A	N/A
$\beta(10)$	N/A	N/A
$\beta(11)$	N/A	N/A
$\beta(12)$	N/A	N/A
% AAD − P	2.011	1.5112
% AAD − v^{liq}	1.001	0.7036
% AAD − v^{vap}	4.8646	4.8117

Table 3. Parameter Values for Pure Water Association Schemes

parameter	1−2	no association
T_C' (K)	287.4298	307.4124
P_C' (bars)	30.8158	27.5985
ω'	2.6850×10^{-2}	3.6655×10^{-2}
B (cc/mol)	16.0698	21.6812
ΔH^0 (J/mol)	−22870.44	N/A
ΔC_P° (J/(mol K))	0.0	N/A
ΔS^0 (J/(mol K))	−167.8223	N/A

Pure Water. Several available models for water treat it as a mixture of different types of clusters.[28,36−39] These theories do not provide any conclusive information on the types of clusters that could be included to develop association-based equation of state models for water. Therefore, two different schemes were considered for water. First, the most simplistic association scheme that allows the formation of monomers and dimers only. Second, to demonstrate the effect of association in water, a model with no association interaction was also included. The values of the parameters for these two association schemes are listed in Table 3.

Figure 4 shows the vapor pressure and saturated liquid and vapor volumes from the two different schemes used for water. As can be seen, even an association scheme as simple as a monomer−dimer type shows high correlative ability. Also, the effect of association is pronounced in the liquid-phase volume, where the no-association case shows large deviations from the experimental values, corroborating the limited association that is exhibited by water in the vapor phase. The reason for representing the water association only by a monomer−dimer scheme was 2-fold. First, the simplicity of the monomer−dimer scheme is advantageous

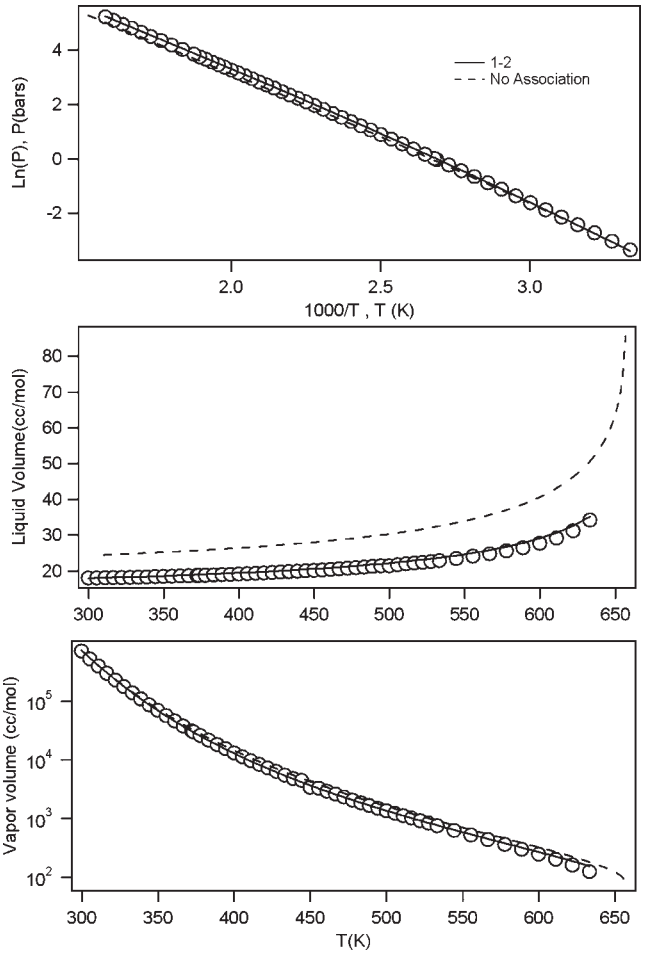

Figure 4. Pure water VLE results relative to experimental data.[56]

during the extension to mixtures, as it offers a closed form expression. Second, in the binary (HF + H_2O) mixture, the overwhelming importance of HF self-association dominates the attractive interactions and hence, for water, a 1−2 association scheme is a reasonable starting point. The effect of using a monomer−dimer and a continuous infinite association scheme for water was previously explored by Prausnitz et al.,[24] where they deem that the level of accuracy a simple analytic equation of state of this kind provides is desirable especially from a computational efficiency standpoint.

Pure HF Predictions. During the correlation stage of the model, the association schemes that were used to describe pure HF included the experimental vapor pressure and the saturated-phase volumes only. However, to evaluate the different association schemes, it is essential to study the predictive ability of each scheme. To address this, several pure component properties of HF were predicted using the parameter set that was obtained during the correlation stage of the model.

The predictive ability of all the association schemes for pure HF is discussed in the next few sections. First, the heat of vaporization results for pure HF from various schemes are discussed. This is followed by the constant pressure heat capacity, constant volume heat capacity, $P-v$ isotherms (supercritical and superheated vapor region), and isothermal liquid-phase density data. Almost all available relevant experimental data for pure HF are reported at multiple operating conditions. While the

predictive ability of the various schemes, sometimes with multiple parameter sets of the same scheme, were studied for all experimental conditions, the results are plotted only for a few schemes for ease of visualization. However, the deviations from the experimental data for all schemes and for all available experimental conditions are provided at the appropriate sections.

Heat of Vaporization. The enthalpy (H) of any fluid is written conveniently in terms of ideal and residual gas contributions as[40]

$$H(T,P) = H^{IG}(T) + H^{r}(T,P) \quad (9)$$

For pure HF, the ideal gas part of the enthalpy (H^{IG}), is obtained from statistical mechanics by applying rigid rotor/harmonic oscillator approximations and is given by[41]

$$H^{IG}(T) = \frac{7}{2}R(T - T^0) + R\theta\left(\frac{1}{\exp(\theta/T) - 1} - \frac{1}{\exp(\theta/T^0) - 1}\right) \quad (10)$$

where θ is the characteristic temperature of vibration (5955.16 K for HF).

The residual part of the enthalpy, $H^{r}(T,P)$, can be written as[42]

$$H^{r} = RT(Z - 1) + \int_{v}^{\infty}\left[P - T\left(\frac{\partial P}{\partial T}\right)_{v}\right] dv \quad (11)$$

This is more conveniently expressed in terms of chemical and physical contributions. The physical part of the residual enthalpy (PREOS) can be written as

$$H^{r(ph)} = \frac{1}{2\sqrt{2}B}\left[A(T) - T\left(\frac{dA}{dT}\right)\right]\ln\left[\frac{v + B(1 - \sqrt{2})}{v + B(1 + \sqrt{2})}\right] \quad (12)$$

The chemical part of the residual enthalpy is given by

$$H^{r(ch)} = [\Delta C_p^0(T^0 - T) - \Delta H^0 - RT](Z^{ch} - 1) \quad (13)$$

The complete residual enthalpy is given by

$$H^{r} = H^{r(ph)} + H^{r(ch)} + RT(Z - 1) \quad (14)$$

The heat of vaporization (ΔH_{vap}) is calculated as the difference between the vapor- and liquid-phase enthalpies along the saturation curve. The predicted results from various association schemes are shown in Figure 5. As one can see, the temperature at which the unusual peak in the heat of vaporization occurs is best captured by the 1−4 scheme. However, the level of accuracy of this scheme fails at higher temperatures.

For HF it is important to achieve accuracy both in the specification of the oligomers and in their distribution. Hence, multiple parameter sets with the same set of oligomers but different oligomer distributions could provide different results. To demonstrate this, for all the pure HF predicted properties, the results from the 1−2−6−8 scheme are reported for two different parameter sets (cases 1 and 2 from Table 3). For the ΔH_{vap} of pure HF, both cases 1 and 2 are reported to predict this property with the same level of accuracy, with case 1 showing slightly lower deviations from the experimental data than case 2 near the critical point. This supports the notion of the importance of a correct distribution of the oligomers in this mixture.

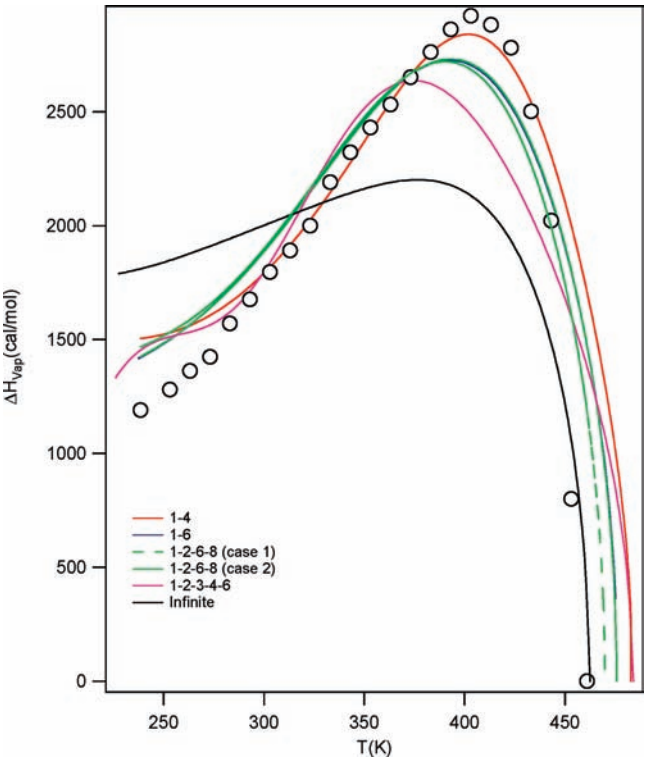

Figure 5. Pure HF heat of vaporization predicted by different association schemes relative to experiment.[45]

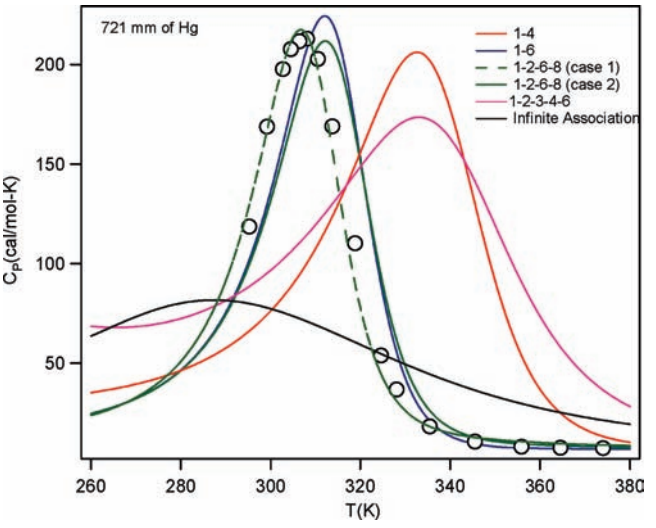

Figure 6. Superheated vapor heat capacity for pure HF predicted by different association schemes relative to experiment.[45]

Constant Pressure Heat Capacity (C_P). Since the closed-form expressions for Z^{ch} were not available for most of the association schemes, the heat capacity, $C_P = (\partial H/\partial T)_P$, was calculated numerically from the corresponding enthalpy values using a three-point forward difference formula. Figure 6 shows the predicted C_P results from various association schemes. The constant pressure heat capacity for HF has been reported to go through a maximum in the superheated vapor (SHV) region.[43] This unusual C_P peak in HF is well captured by most of the

dx.doi.org/10.1021/je1011955 |J. Chem. Eng. Data 2011, 56, 1506–1525

association schemes shown in Figure 5. The 1−4 association scheme, which was reported to be the best in predicting ΔH_{vap} values, predicts the magnitude of the C_P reasonably but fails to predict the temperature at which the peak occurs. The 1−2−6−8 (case 1) scheme predicts the temperature as well as the magnitude well when compared to the other schemes. Case 2 of the same 1−2−6−8 association scheme was reported to overpredict the temperature at which the peak occurs and underpredict the magnitude of the C_P peak when compared to the experimental data. The infinite association scheme predicts the C_P in the SHV region poorly when compared to other schemes reported in Figure 6.

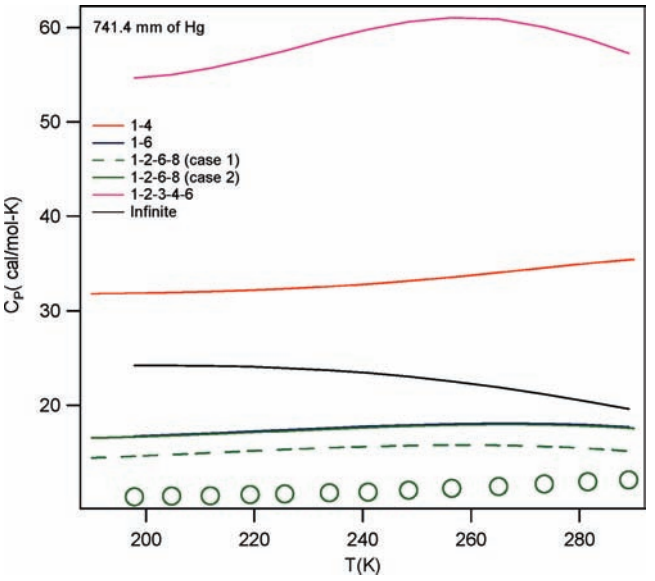

Figure 7. Liquid-phase heat capacity for pure HF predicted by different association schemes relative to experiment.[44]

The liquid-phase C_P results relative to the experimental data reported by Hu et al.[44] at 741.44 mmHg are shown in Figure 7. As one can see, almost all schemes predict the liquid-phase C_P poorly. The 1−6 and 1−2−6−8 (case 1) schemes were reported to be the most reasonable when compared with the other schemes shown in Figure 7. Also, the 1−2−6−8 (case 1) was reported to show better results in comparison with case 2 of the same association scheme.

The % AAD values for all the association schemes for ΔH_{vap}, the superheated vapor C_P at all available experimental conditions, and the liquid-phase C_P at 741.44 mmHg are listed in Table 4. From the % AAD it can be seen that the schemes that predict the ΔH_{vap} as well as the C_P at a reasonable level of accuracy when compared to other schemes reported here were, 1−6, 1−2−6, 1−2−6−8 (cases 1 and 2), 1−2−3−6−9, 1→9, and 1→12. For the rest of this paper, in the tabulations, the best performing schemes based on % AAD values are shown in boldface.

Constant Volume Heat Capacity. Figure 8 shows the constant volume heat capacity results, $C_v = (\partial U/\partial T)_v$, which was also calculated numerically using a three-point formula. As one can see, none of the schemes reported here predicts this property accurately. The 1−4 association scheme was reported to predict C_v at a reasonable level of accuracy at superheated vapor regions when compared to the other schemes. However, the liquid-phase C_v predicted by this scheme was poor when compared to the other association schemes. This is illustrated by the % AAD values listed in Table 5 for different association schemes for all available experimental conditions. Similar to C_P, the association schemes that were reported to be relatively reasonable in predicting C_v at all available experimental conditions were the 1−6, 1−2−6, 1−2−6−8 (cases 1 and 2), 1−2−3−6−9, 1→9, and 1→12 schemes.

***P*−*v* Isotherm: Supercritical Region.** The experimental supercritical $P-v$ isotherms for pure HF were reported from two different studies.[45,46] Even though some of the reported supercritical temperature conditions overlap in both these data

Table 4. % AAD Values for the Predicted ΔH_{vap}, C_P (Superheated Vapor, Liquid) of Pure HF from Different Association Schemes

		C_P (at mmHg)							
		superheated vapor							liquid
scheme	ΔH_{vap}	721	623	519	420	319	230	116	741.4
1−2	56.89	132.47	123.24	140.70	130.69	142.06	161.03	160.39	**27.08**
1−4	**12.18**	257.38	252.18	270.26	219.46	223.41	261.09	311.37	202.18
1−6	13.42	**20.89**	**28.23**	**27.18**	**23.03**	**27.29**	**22.98**	**25.68**	60.19
1−2−3	21.60	343.31	292.90	373.86	301.49	383.57	434.39	335.34	49.43
1−2−6	**12.70**	29.99	35.26	35.55	27.90	29.42	29.47	29.73	56.77
1−3−6	**13.08**	**23.11**	**29.97**	**29.05**	**23.68**	**25.53**	**23.92**	**24.95**	55.51
1−2−12	**13.01**	62.99	63.32	67.57	65.74	70.10	72.12	67.63	**20.55**
1−2−6−8 (case 1)	**12.78**	**11.41**	**10.12**	**11.56**	**12.57**	**12.78**	**15.49**	**19.00**	**39.98**
1−2−6−8 (case 2)	**12.98**	26.53	32.32	32.24	25.25	**26.65**	26.31	26.70	59.20
1−2−3−4−5	15.63	285.07	254.01	312.71	240.88	300.96	352.45	324.42	302.65
1−2−3−4−6	13.54	318.00	287.00	354.90	272.43	347.44	412.36	378.38	430.93
1−2−3−6−9	**12.99**	26.64	**27.51**	**26.96**	30.63	30.31	31.10	37.45	**40.94**
1→9	**12.83**	**10.85**	**10.15**	**12.18**	**8.03**	**8.74**	**12.58**	**12.23**	50.80
1→12	13.85	**13.20**	**11.84**	**13.41**	**13.88**	**14.28**	**17.02**	**18.26**	74.35
∞	24.17	64.56	65.87	63.70	67.82	62.81	59.89	61.48	108.97

dx.doi.org/10.1021/je1011955 |*J. Chem. Eng. Data* 2011, 56, 1506–1525

sets, the % AAD values are listed as two separate data sets in Tables 6 and 7. The supercritical $P-v$ isotherm for pure HF at 573 K from various association schemes relative to experiment[46] is shown in Figure 9. From the % AAD values listed in Table 7, it can be seen that the association schemes that were reported to be reasonable in predicting the properties that were discussed earlier were also predictive here. On the other hand, the 1−2−12 and the 1−3−6 association schemes predict this property more accurately than the properties explored in the previous section. The infinite association scheme shows fair agreement at temperatures moderately above the critical point but fails at higher temperatures. Also, the 1−2−6−8 case 1 parameter set reported lesser deviations from the experimental values than the case 2. The association schemes that were relatively poor in predicting this property were 1−2, 1−4, 1−2−3, 1−2−3−4−5, and 1−2−3−4−6.

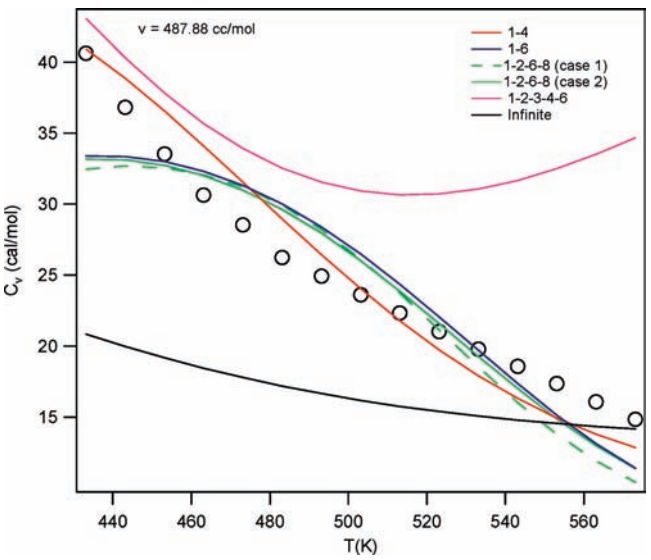

Figure 8. C_v results for pure HF predicted by different association schemes relative to experiment.[45]

Isothermal Compressibility Factor (Z): Superheated Vapor. In Figure 10, the isothermal compressibility factor, Z, at the superheated vapor region from various association schemes is shown relative to the experimental data at 299.15 K.[45] The 1−4, 1−2−3−4−6, and infinite association schemes show poor predictions at this condition when compared to the 1−6 and 1−2−6−8 schemes. The % AAD values for this property that are listed in Table 8 are reported with similar predictive agreement with the properties that are discussed in the previous sections.

Isothermal Densities of Liquid HF. The density predictions from different association schemes for pure HF, relative to the experimental data at 293.55 K,[47] are shown in Figure 11 (shown as volumes). The % AAD values for all the experimental conditions from all association schemes are listed in Table 9. At 293.55 K, the 1−2−6−8 association scheme (case 2) was reported to predict the best when compared to the other association schemes. The other association schemes that predict this property with a reasonable accuracy are 1−6, 1−2−6, and 1−3−6, respectively. The 1−2, 1−2−12, 1−2−3−6−9, and infinite association schemes were reported to predict this property poorly when compared to other schemes. Also, case 2 of the 1−2−6−8 association scheme was reported to predict this property better than the case 1 of the same association scheme.

PURE HF CONCLUDING REMARKS

Several pure component association schemes that were used to correlate and predict the bulk-phase properties of pure HF were reported with varying degrees of success. Even though it is not quite possible to pick one particular association scheme to be the best in correlating and predicting all of these properties for pure HF, a few of them can be considered to be reasonably accurate. From the reported % AAD values of the various properties from Tables 4−9, over a large range of operating conditions, the 1−6, 1−2−6, 1−2−6−8 (cases 1 and 2), 1−2−3−6−9, 1→9, and 1→12 schemes can be considered as reasonable and the poorest association schemes were 1−2, 1−4, 1−2−3−4−5, and 1−2−3−4−6. The

Table 5. % AAD Values for the Predicted C_v of Pure HF from Different Association Schemes

	C_V at corresponding volumes (cc/mol)														
scheme	487	285	186	150	121	96	81	74	67	49	40	33	27	23	20
1−2	77.64	78.08	77.35	76.20	74.58	71.96	69.72	68.00	66.38	60.66	56.89	53.29	46.19	34.78	14.48
1−4	**8.49**	**5.63**	**13.66**	19.42	26.10	37.87	49.16	57.64	65.37	90.48	107.52	122.97	101.04	80.50	153.36
1−6	**10.66**	**13.34**	**16.97**	**17.31**	**18.50**	**18.45**	**17.66**	**17.17**	**16.59**	21.56	25.88	**23.83**	**24.83**	32.21	**22.00**
1−2−3	29.62	24.27	23.45	23.69	25.06	25.52	25.08	25.03	25.57	30.99	32.38	30.33	**25.65**	**20.41**	**19.93**
1−2−6	**11.14**	**13.20**	**17.36**	**17.84**	**19.09**	**19.27**	**18.51**	**18.06**	**17.42**	22.31	26.55	24.43	26.77	36.65	**22.71**
1−3−6	**10.83**	**14.03**	**17.60**	**17.94**	**19.08**	**18.96**	**18.08**	**17.48**	**16.83**	21.32	25.52	23.58	26.65	37.03	**22.36**
1−2−12	21.90	**11.61**	20.97	21.57	22.44	21.50	19.70	18.29	**17.08**	**17.60**	**20.37**	**21.69**	42.13	62.17	31.04
1−2−6−8 (case 1)	**12.64**	**15.56**	19.97	20.15	21.15	20.65	19.22	18.23	**17.35**	**19.88**	**23.33**	**22.24**	36.84	55.24	**26.28**
1−2−6−8 (case 2)	**10.46**	**12.98**	**16.99**	**17.41**	**18.65**	**18.67**	**17.90**	**17.44**	**16.86**	21.82	26.19	**24.12**	**25.88**	**34.63**	**22.50**
1−2−3−4−5	19.98	26.91	34.45	41.05	48.90	63.02	74.20	82.68	90.20	113.00	125.44	135.36	155.51	178.49	215.11
1−2−3−4−6	45.76	53.81	63.40	72.20	83.66	100.45	113.56	123.51	132.28	158.77	170.34	174.21	191.44	221.67	294.21
1−2−3−6−9	**11.95**	**13.09**	18.66	19.06	**20.13**	19.59	**18.23**	**17.12**	**16.33**	**19.01**	**22.75**	**22.02**	35.92	53.70	25.68
1→9	**11.07**	**14.45**	19.08	19.29	**20.45**	20.15	18.95	18.07	**17.30**	**20.51**	24.31	**22.84**	35.45	53.05	26.12
1→12	**10.10**	**12.61**	**17.45**	**17.75**	18.44	**17.85**	**16.85**	**16.02**	**15.50**	**19.83**	**23.69**	**20.36**	**24.05**	32.77	**21.80**
∞	29.70	29.01	27.03	24.81	22.90	20.70	19.02	**17.89**	**17.32**	21.73	**23.01**	**14.18**	**11.83**	**13.39**	35.23

dx.doi.org/10.1021/je1011955 |J. Chem. Eng. Data 2011, 56, 1506–1525

Table 6. % AAD Values for the Predicted Supercritical $P-v$ Isotherms for Pure HF from Different Association Schemes

	$P-v$ isotherms at supercritical conditions[50] (at T (K))										
scheme	473	523	573	623	673	723	773	823	873	923	973
1−2	128.63	50.95	34.83	32.61	31.80	32.18	38.57	45.77	50.10	56.46	62.14
1−4	63.56	31.86	10.82	15.13	20.38	26.95	36.89	43.23	46.62	51.18	54.49
1−6	29.50	**14.80**	**2.64**	**4.56**	**7.68**	11.28	13.71	15.23	16.99	18.42	18.26
1−2−3	70.32	40.16	17.25	17.64	19.37	18.49	13.42	**10.99**	**10.02**	**7.12**	**5.91**
1−2−6	30.63	16.61	4.38	**2.04**	**4.73**	**8.29**	**10.32**	**11.50**	**12.85**	13.90	13.47
1−3−6	30.75	16.13	**3.59**	**2.94**	**5.54**	**8.99**	**11.03**	12.18	13.48	14.56	14.00
1−2−12	**5.69**	**8.00**	**6.89**	11.35	13.10	15.16	13.39	11.78	**11.31**	**10.18**	**8.25**
1−2−6−8 (case 1)	**18.34**	**10.15**	**3.15**	**3.10**	**5.84**	**8.84**	**9.62**	**9.80**	**10.38**	**10.72**	**10.11**
1−2−6−8 (case 2)	30.82	16.17	**3.51**	**3.49**	**6.39**	**9.96**	12.33	13.78	15.48	16.84	16.57
1−2−3−4−5	52.87	24.42	16.85	19.31	21.22	22.45	26.62	31.28	32.41	36.55	39.84
1−2−3−4−6	58.20	36.56	20.36	20.81	20.66	20.67	19.82	22.75	25.51	31.70	36.83
1−2−3−6−9	**10.21**	**4.15**	**2.53**	**7.08**	**9.56**	12.67	**12.95**	**13.05**	13.89	**13.97**	**12.71**
1→9	21.06	12.43	**3.98**	**2.28**	**5.24**	**8.66**	**9.85**	**10.32**	**11.14**	**11.58**	**10.96**
1→12	**16.65**	**7.73**	**3.04**	10.12	14.50	19.12	22.43	24.77	27.06	29.07	29.64
∞	**2.57**	**5.13**	7.94	10.18	16.65	24.55	33.68	40.66	45.35	50.74	54.81

Table 7. % AAD Values for the Predicted Supercritical $P-v$ Isotherms for Pure HF from Different Association Schemes

	$P-v$ isotherms at supercritical conditions (at T (K))											
scheme	463	473	483	493	503	513	523	533	543	553	563	573
1−2	47.14	42.85	39.01	36.94	35.63	34.92	34.57	36.06	36.21	36.39	36.23	36.63
1−4	15.17	8.08	**5.89**	7.15	8.11	8.97	9.88	10.85	12.73	14.51	17.18	18.84
1−6	**10.67**	**5.30**	**5.60**	**5.77**	**5.59**	**5.28**	**4.97**	**4.52**	**4.59**	**4.82**	5.53	5.95
1−2−3	27.17	22.57	18.72	15.91	14.20	12.83	11.66	10.63	9.53	8.48	8.53	7.72
1−2−6	**10.93**	**4.66**	**4.39**	**4.74**	**4.60**	**4.17**	3.75	**2.90**	**3.03**	**3.17**	**3.66**	**4.01**
1−3−6	**10.83**	**5.05**	**5.16**	**5.33**	**5.18**	**4.74**	**4.33**	**3.73**	**3.75**	**3.85**	**4.55**	**4.91**
1−2−12	11.47	**5.79**	**5.21**	**4.89**	**4.29**	**3.99**	**4.05**	**4.41**	**4.70**	**4.96**	**4.86**	**5.03**
1−2−6−8 (case 1)	**9.94**	**3.98**	**4.96**	**5.06**	**4.71**	**4.08**	**3.63**	**2.90**	**2.71**	**2.74**	**3.00**	**3.30**
1−2−6−8 (case 2)	**10.84**	**5.13**	**5.30**	**5.47**	**5.37**	**4.97**	**4.65**	**3.98**	**4.04**	**4.04**	**4.79**	**5.19**
1−2−3−4−5	18.93	17.57	19.08	20.75	22.23	23.63	25.02	28.78	30.37	31.84	35.28	36.67
1−2−3−4−6	17.78	15.66	16.50	18.18	19.69	21.21	22.68	24.93	26.51	28.02	32.53	33.99
1−2−3−6−9	**10.50**	**4.91**	**5.81**	**5.92**	**5.61**	**5.04**	**4.50**	**4.17**	**4.12**	**4.28**	**4.83**	**5.13**
1→9	**10.24**	**4.33**	**5.26**	**5.46**	**5.20**	**4.65**	**4.07**	**3.10**	**2.85**	**2.85**	**3.09**	**3.40**
1→12	11.46	6.76	8.16	8.52	8.55	8.44	8.33	8.63	8.89	9.24	10.20	10.44
∞	17.77	14.95	17.16	18.72	19.87	20.82	21.70	24.10	24.95	25.74	29.65	30.68

predictive behavior of these association schemes supports the spectroscopic evidence on the existence of specific oligomers, such as hexamers, for pure HF.

Also, the existence of multiple parameter sets for the same association scheme with varying degrees of accuracy in predicting the pure HF properties demonstrated the importance of capturing the accurate distribution of these oligomers. It is important to explore the parameter space completely for all available physically meaningful parameter sets that show minimum deviations from the experimental data. Accordingly, similar to the analysis on the 1−2−6−8 association scheme, the existence of the multiple parameter sets and their correlative and predictive ability were explored for all other schemes. Two different parameter sets for the 1−2−6, 1−3−6, and 1−2−3−6−9 association schemes; four different parameter sets for the 1→9 and 1−2−6−8 association schemes were identified. The parameters reported in Table 1 were the best based on the correlative and predictive ability of the parameter set in comparison with the others.

Note that in this work we do not examine the predictive behavior of the pure water models. This is mainly because we have focused on the notion that HF self-association dominates the interactions in HF mixtures. Accordingly, for water, a relatively simple pure component model with good correlative behavior is sufficient at this level. However, a more descriptive association model in this methodology should study the predictive behavior of both pure components in detail.

HF−H_2O Mixture Association Model. In one of the earlier works on this mixture,[26] a continuous association scheme with increased probability of the occurrence of hexamers was used for pure HF with water considered to be inert. The correlated-phase equilibrium property results from this model, hereafter called the

dx.doi.org/10.1021/je1011955 |J. Chem. Eng. Data 2011, 56, 1506–1525

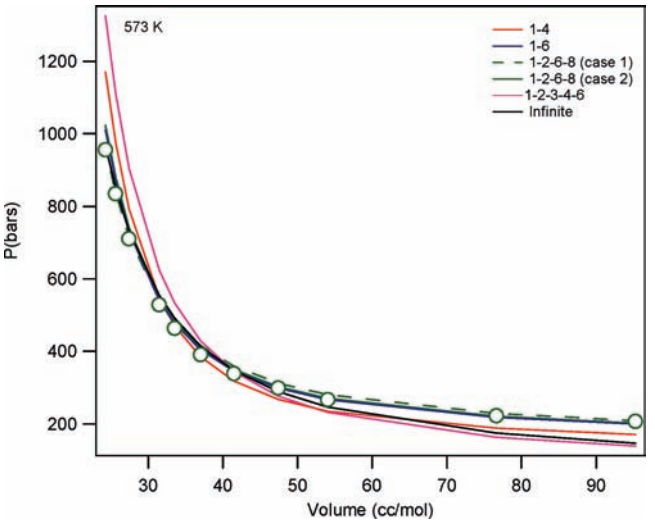

Figure 9. Supercritical $P-v$ isotherm for pure HF at 573 K predicted by different association schemes relative to experiment[46].

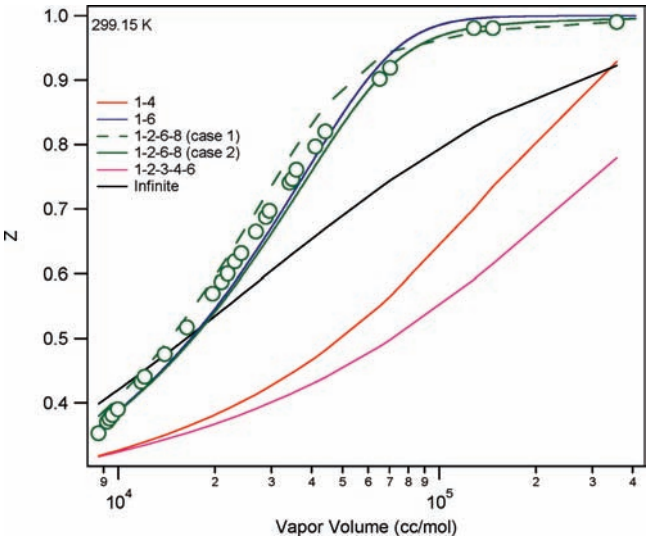

Figure 10. Superheated vapor isothermal Z for pure HF at 299.15 K predicted by different association schemes relative to experiment.[57]

AEOS-VK model, indicated that the association interactions specified in the model were not sufficient to describe the complex interactions that are occurring in this system. This section describes the development of an association model for aqueous HF mixtures. The effect of the inclusion of different types of association interactions in the binary mixture is studied in two different ways. The mixture is initially considered to show only self-association interactions through the pure component models that were discussed in the pure component part of this paper, with no inclusion of cross-association between the species. Next, the effect of the inclusion of cross-association is also studied. In both cases, similar to the pure components, the correlative and predictive ability of the respective association schemes are also discussed.

Formulation of the Mixture Association Model. While developing the AEOS-VK model for binary mixtures of HF, the non-HF species in the mixture were assumed to show no association interactions.[26] Hence, while extending it to a binary mixture containing HF, the chemical part of the compressibility factor Z^{ch} was defined as

$$Z^{ch} = X_{HF} f(q_{HF}) + (1 - X_{HF}) \tag{15}$$

where $q_{HF} = RTK^{HF}X_{HF}/v$, with K^{HF} being the dimerization constant for HF and X_{HF} is the apparent mole fraction of HF in the binary mixture. Here, the apparent mole fraction is the nominal concentration of the species in solution (i.e., mole fraction of HF in a binary mixture of HF + H_2O), and the concentration of a particular species (say a dimer or trimer) in the solution is defined as the true mole fraction. In eq 15, the function f is the association scheme that was used to describe HF in the AEOS-VK formulation. However, for association schemes with no analytical formulation, eq 15 is modified as

$$Z^{ch} = X_{HF} Z^{ch}_{HF} + (1 - X_{HF}) \tag{16}$$

In eq 15, Z^{ch}_{HF} is calculated numerically as a function of the number of moles of individual oligomers that are present in the association scheme that is adopted to describe HF as in eq 3.

If both species in the binary mixture are assumed to be associating, then eq 14 is modified as[31]

$$Z^{ch} = X_{HF} f(q_{HF}) + X_{H_2O} g(q_{H_2O}) \tag{17}$$

where $q_{H_2O} = RTK_{H_2O}X_{H_2O}/v$ and the functions f and g represent corresponding association schemes for HF and H_2O, respectively. In eq 17, the functions f and g could be same or different depending upon the scheme that is used to describe the pure component association. While this formulation in eq 17 is for association schemes with closed form expressions, for schemes without such analytical formulations, the functions are replaced by the corresponding numerical schemes, Z^{ch}_{HF} and $Z^{ch}_{H_2O}$.

Numerical Formulation of Z^{ch} for Mixtures: Self-Association. The Z^{ch} for a binary mixture with only self-association interactions between the species is obtained in a similar fashion as in the pure component, and is shown as

$$Z^{ch} = \frac{\sum_{i=1}^{M} n_i^{HF} + \sum_{j=1}^{N} n_j^{H_2O}}{\sum_{i=1}^{M} i n_i^{HF} + \sum_{j=1}^{N} j n_j^{H_2O}} \tag{18}$$

where the numerator of eq 18 signifies the total number of moles of HF and water species present (n_T), while the denominator is the total number of moles of HF and water species that would be present (n_0) if there is no association interaction. Similar to the pure component formulation that was described earlier, it can be shown that[31]

$$Z^{ch} = \frac{\sum_{i=1}^{M} K_i^{HF}[Px_{HF}]^i + \sum_{j=1}^{N} K_j^{H_2O}[Px_{H_2O}]^j}{\sum_{i=1}^{M} iK_i^{HF}[Px_{HF}]^i + \sum_{j=1}^{N} jK_j^{H_2O}[Px_{H_2O}]^j} \tag{19}$$

dx.doi.org/10.1021/je1011955 |J. Chem. Eng. Data 2011, 56, 1506–1525

Table 8. % AAD Values for the Isothermal *Z* for Pure HF from Different Association Schemes

	Z at isothermal conditions *T* (K)												
scheme	299.15	305.15	311.15	273.15	286	299	305	211	299.15	305.15	311.15	317.15	329.15
1−2	23.88	20.28	28.84	51.01	13.98	15.65	22.57	27.34	28.15	29.20	27.18	31.32	28.04
1−4	29.60	31.88	31.92	17.50	30.13	37.16	36.69	34.62	29.53	23.54	25.92	20.79	8.19
1−6	**2.96**	**3.12**	**2.00**	**1.07**	**0.98**	**1.04**	**0.97**	**1.81**	**1.73**	**1.55**	**1.51**	**1.39**	**2.81**
1−2−3	33.24	42.87	48.11	5.79	24.18	42.18	45.85	47.95	48.21	46.20	46.02	46.41	38.49
1−2−6	**3.75**	**3.02**	**3.08**	**0.92**	**2.30**	**2.79**	**2.07**	**1.44**	**1.45**	**1.63**	**1.58**	**0.91**	**1.44**
1−3−6	**3.21**	**3.05**	**2.23**	**1.34**	**1.17**	**1.50**	**1.14**	**1.15**	**1.64**	**1.65**	**1.56**	**1.17**	**2.49**
1−2−12	12.62	10.14	**4.95**	25.59	28.35	16.85	9.39	**3.56**	6.95	4.37	6.49	4.64	**3.31**
1−2−6−8 (case 1)	**3.35**	**2.91**	**2.50**	**0.89**	**1.67**	**2.06**	**1.51**	**1.04**	**1.34**	**1.48**	**1.39**	**0.84**	**1.75**
1−2−6−8 (case 2)	**4.08**	4.71	**2.10**	9.94	9.52	**8.31**	7.20	5.78	**1.97**	**1.47**	**1.91**	**0.58**	**1.14**
1−2−3−4−5	31.13	34.98	36.49	16.77	29.86	38.52	39.01	38.12	35.38	30.31	31.92	28.60	17.50
1−2−3−4−6	33.59	37.40	38.59	19.35	32.56	41.12	41.39	40.21	38.83	32.49	34.61	30.32	18.03
1−2−3−6−9	6.58	6.17	**2.72**	14.04	14.60	11.43	8.67	5.67	**2.87**	**1.94**	**2.67**	**0.85**	**0.40**
1→9	**2.68**	**3.30**	**1.14**	**8.47**	**7.50**	**6.05**	**5.16**	**4.13**	**1.26**	**0.75**	**1.14**	**0.22**	**1.06**
1→12	**4.66**	**5.19**	**2.34**	9.69	9.98	**8.88**	7.64	6.04	**2.09**	**1.58**	**2.10**	**0.56**	**1.26**
∞	10.97	13.02	18.68	17.78	4.23	11.20	15.44	18.28	14.06	15.56	14.18	16.75	12.35

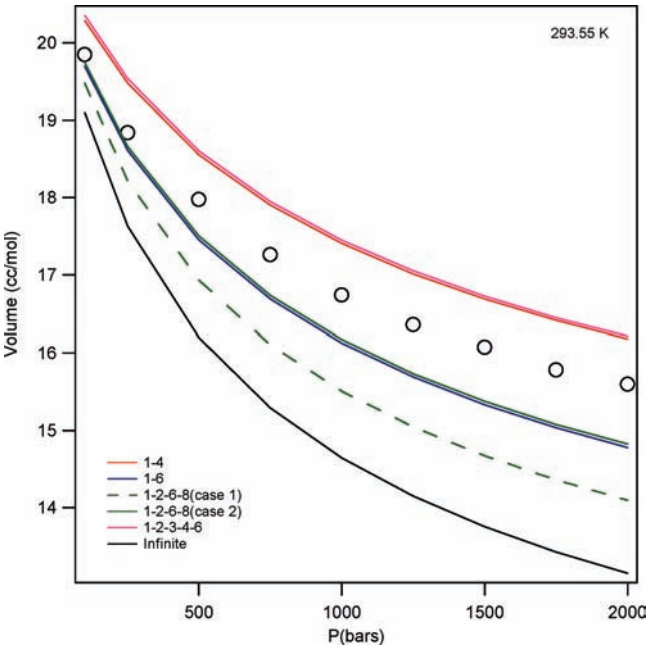

Figure 11. Isothermal density for pure HF at 293.55 K predicted by different association schemes relative to experiment.[47]

In eq 19, K_i^{HF} and $K_j^{H_2O}$ represent the corresponding *i*-mer and *j*-mer equilibrium constants for HF and water, with *M* and *N* being the maximum number of oligomers that are allowed to be formed in the association schemes that are used. $Px_{HF} = [(RTZ^{ch}/v)z_{HF(1)}]$ and $Px_{H_2O} = [(RTZ^{ch}/v)z_{H_2O(1)}]$, with $z_{HF(1)}$ and $z_{H_2O(1)}$ representing their respective monomer mole fractions. As in the pure component models, based on a material balance, it can be shown that[31,48]

$$\frac{RT}{v} = \sum_{i=1}^{M} iK_i^{HF}[Px_{HF}]^i + \sum_{j=1}^{N} jK_j^{H_2O}[Px_{H_2O}]^j \qquad (20)$$

From eqs 18 and 19, it is possible to obtain the apparent mole fraction X_{HF} and X_{H_2O} as shown below,

$$X_{HF} = \frac{\sum_{i=1}^{M} iK_i^{HF}[Px_{HF}]^i}{\sum_{i=1}^{M} iK_i^{HF}[Px_{HF}]^i + \sum_{j=1}^{N} jK_j^{H_2O}[Px_{H_2O}]^j} \qquad (21)$$

$$X_{H_2O} = \frac{\sum_{j=1}^{N} jK_j^{H_2O}[Px_{H_2O}]^j}{\sum_{i=1}^{M} iK_i^{HF}[Px_{HF}]^i + \sum_{j=1}^{N} jK_j^{H_2O}[Px_{H_2O}]^j} \qquad (22)$$

For the association schemes without closed-form expressions, Z^{ch} is obtained via eq 19. In this equation, for a chosen association scheme and for a given condition of *T*, *v*, and X_{HF} (or X_{H_2O}), the unknowns in the equations are Px_{HF} and Px_{H_2O}. These unknowns are obtained by solving them using eqs 20 and 21 (or 22, since $1 - X_{HF} = X_{H_2O}$). Once the numerical values of Px_{HF} and Px_{H_2O} are obtained, they are substituted back into eq 18 to obtain Z^{ch}. This process is repeated for each condition of *T*, *v*, and X_{HF} (or X_{H_2O}) across the entire composition of the binary mixture.

Z^{ph} for Mixtures. The physical part of the compressibility factor was included via the Peng−Robinson equation of state[30] with the pure component parameters as described earlier. However, for mixtures, it is essential to incorporate the composition dependency of the equation of state parameters using appropriate mixing rules. To model the complex phase behavior of mixtures, various mixing rules have been proposed,[49,50] and here a one-parameter (θ_{ij}) van der Waal mixing rule (VDWMR) was used to describe the mixture equation of state parameters.

Fugacity Coefficient of the Mixture Model. The relationship used to derive these fugacity coefficient when the volumetric data are given in pressure-explicit form is[51]

$$\ln \phi_i = \frac{1}{RT}\int_V^{\infty} \left[\left(\frac{\partial P}{\partial n_i}\right)_{T,V,n_j} - \frac{RT}{V}\right] dV - \ln Z \qquad (23)$$

Table 9. % AAD Values for the Isothermal Densities for Pure HF from Different Association Schemes

	densities at isothermal conditions T (K)						
scheme	258.6	268.8	278.7	293.5	317.8	342.9	373.9
1−2	15.14	16.37	16.11	15.30	15.13	16.11	15.49
1−4	**3.76**	**4.12**	**4.09**	**3.58**	**3.54**	4.24	**3.38**
1−6	**2.61**	**2.88**	**2.86**	**3.39**	**3.52**	2.90	**3.54**
1−2−3	7.91	8.51	8.22	7.40	7.12	7.94	7.36
1−2−6	**2.47**	**2.77**	**2.73**	**3.27**	**3.44**	**2.85**	**3.52**
1−3−6	**2.38**	**2.70**	**2.64**	**3.17**	**3.32**	**2.74**	**3.38**
1−2−12	13.09	**14.09**	14.13	14.65	14.96	14.65	15.39
1−2−6−8 (case 1)	5.48	6.03	6.12	6.72	7.02	6.60	7.35
1−2−6−8 (case 2)	**2.32**	**2.66**	**2.60**	**3.13**	**3.29**	**2.71**	**3.36**
1−2−3−4−5	**3.87**	**3.91**	**3.63**	**2.83**	**2.58**	**3.44**	**3.11**
1−2−3−4−6	5.84	5.45	4.94	**3.84**	**3.14**	**3.58**	**2.87**
1−2−3−6−9	7.58	8.29	8.39	8.98	9.34	8.99	9.78
1−2−3−6−9(2)	6.52	7.25	7.39	8.05	8.48	8.18	8.99
1→9	4.70	5.25	5.35	5.98	6.32	5.93	6.71
1→12	5.28	5.93	6.08	6.75	7.12	6.71	7.42
∞	7.35	8.92	9.41	11.39	13.76	14.92	16.93

where n_i is the number of moles of species i in the mixture. It is possible to separate the fugacity coefficient into a chemical and physical part by writing Z in terms of a chemical and physical part. Accordingly,

$$\ln \phi_i = \ln \phi_i^{ch} + \ln \phi_i^{ph} - \ln Z \tag{24}$$

where

$$\ln \phi_i^{ch} = \int_V^{\infty} \left[\left(N \left(\frac{\partial Z^{ch}}{\partial n_i} \right)_{T,V,n_j} + Z^{ch} - 1 \right) \right] \frac{dV}{V} \tag{25}$$

and

$$\ln \phi_i^{ph} = \int_V^{\infty} \left[\left(N \left(\frac{\partial Z^{ph}}{\partial n_i} \right)_{T,V,n_j} + Z^{ph} - 1 \right) \right] \frac{dV}{V} \tag{26}$$

Here, $\ln \phi_i^{ph}$ can be written as

$$\ln \phi_i^{ph} = \ln \phi_i^{PR} + \ln Z^{ph} \tag{27}$$

where $\ln \phi_i^{PR}$ is the fugacity coefficient of the Peng−Robinson equation of state and is given by eq 28.

$$\ln \phi_i^{PR} = \frac{b_i}{b}\left(\frac{Pv}{RT} - 1\right) - \ln \frac{P(v-b)}{RT} - \frac{a}{2\sqrt{2}bRT}\left[\frac{2\sum_j X_j a_{ij}}{a} - \frac{b_i}{b}\right] \ln \frac{v + (1+\sqrt{2})b}{v + (1-\sqrt{2})b} \tag{28}$$

where b_i and a_{ij} are the Peng−Robinson equation of state parameters and X_j is the apparent mole fraction of the component "j".

While it is possible to calculate the physical part of the fugacity coefficient through a closed-form expression as specified, it is not so for the chemical part. As suggested earlier, closed-form expressions are not available for most of the association schemes that are used for HF in this study, hence $\ln \phi_i^{ch}$ in eq 25 has to be calculated numerically. However, an analytical formulation can be obtained for the derivative term, $N(\partial Z^{ch}/\partial n_i)_{T,v,n_j}$, in eq 25, and this is shown as

$$N\left(\frac{\partial Z^{ch}}{\partial n_i}\right)_{T,V,n_j} = \sum_{m_i=1}^{M} \frac{(1 - m_i Z^{ch}) m_i \left(\frac{G_i}{K_i}\right)^{m_i - 1} K_{m_i}}{m_i^2 \left(\frac{G_i}{K_i}\right)^{m_i - 1} K_{m_i}} \tag{29}$$

In the above equation, N is the total number of moles (equivalent to n_0 in the Z^{ch} formulation), m_i is number of monomeric units in a corresponding oligomer that are allowed to form in the chosen association scheme, M is the maximum number of oligomers that are allowed to form in the scheme, K_i is the dimerization constant of the corresponding pure component, K_{m_i} is the equilibrium constant for the formation of an oligomer with m_i members, and $G_i = Px_iK_i$. The chemical part of the fugacity coefficient is obtained by integrating eq 25 numerically.

As specified earlier, the phase equilibrium results are obtained for this mixture by solving the corresponding equilibrium constraints, using the equations discussed in this section. Since the pure component parameters are already optimized for vapor pressure and saturated liquid and vapor volumes, the only parameter that has to be optimized for minimum deviations from the mixture experimental data (self-association only) is the binary interaction parameter (θ_{ij}). The next section will discuss the results that are obtained from various mixture self-association schemes.

MIXTURE RESULTS

For pure HF, 14 different pure component association schemes were considered. The phase equilibrium properties of the binary mixture are obtained by considering all 14 different association schemes for HF and with a 1−2 association scheme for water. The binary interaction parameter is optimized for minimum deviation from the experimental $T-x-y$ results.[52−54] While optimizing the θ_{ij}, it was important to achieve a balance in accuracy on both the correlation of the $T-x-y$ data in the region of higher concentrations of HF and the composition at which the azeotrope was reported. All of the self-association schemes showed approximately 1% deviation from the experimental data. The results from the 1−2, 1−4, 1−6, 1−2−6−8, 1−2−3−4−6, and infinite association schemes for HF are shown in Figure 12. The 1−2−6−8 and 1−6 association schemes capture the phase behavior best in comparison with other models. The phase equilibrium properties along the HF rich region and also the azeotropic composition are well captured by these two models. The infinite association model shows the poorest correlation among the reported models in Figure 12. In addition to this, the infinite association scheme also exhibits a phase split at the concentrated HF region (circled in the plot) and reported double azeotrope at dilute HF conditions. The association schemes that show the best correlation are 1−4, 1−6, 1−2−6, 1−3−6, and 1−2−6−8. The θ_{ij} for all these self-association schemes are listed in Table 10.

Even though most of the self-association schemes that were adopted for HF in conjunction with a 1−2 scheme for water are reported to show very good agreement with the experimental $T-x-y$ data at 1 atm for the HF + H_2O system, the binary interaction parameter, θ_{ij}, was for some of these schemes still reported to be highly negative. The AEOS-VK model for this mixture, which used an infinite association model of HF with no inclusion of association interactions for water, was reported with a θ_{ij} value of −1.295. Most of

dx.doi.org/10.1021/je1011955 |J. Chem. Eng. Data 2011, 56, 1506–1525

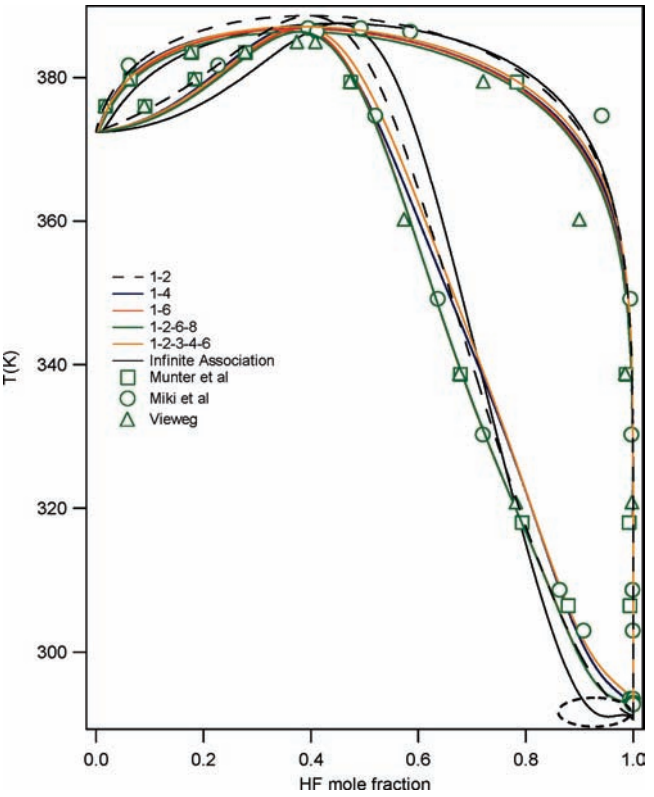

Figure 12. $T-x-y$ results for HF−H_2O system at 1 atm from various self-association models. The experimental data from Miki et al.,[54] Munter et al.,[58] and Vieweg et al.[53] are indicated by empty symbols.

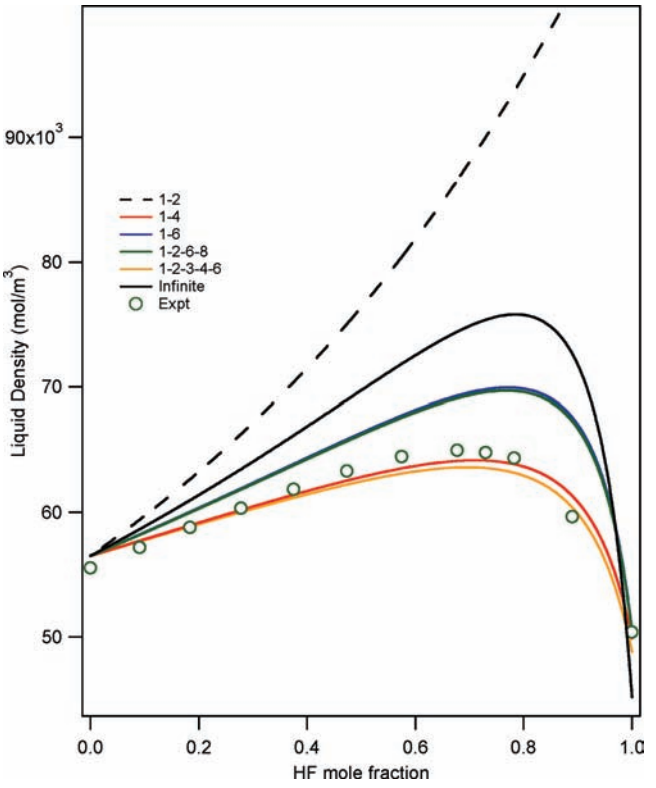

Figure 13. Aqueous HF liquid density predictions from various association schemes relative to the experimental data.[17]

Table 10. Binary Interaction Parameter Values of Self-Association Models

HF scheme	θ_{ij}
1−2	−0.525
1−4	−0.985
1−6	−1.200
1−2−3	−0.690
1−2−6	−1.190
1−3−6	−1.195
1−2−12	−1.460
1−2−6−8	−1.180
1−2−3−4−5	−0.925
1−2−3−4−6	−0.925
1−2−3−6−9	−1.325
1→9	−1.265
1→12	−1.290
∞	−1.225

the self-association schemes used here show some improvement with respect to this θ_{ij} value in comparison to the AEOS-VK model. However, the high negative θ_{ij} value for these schemes is likely indicative of the deficiency of the cross-interactions and also the self-association interactions in H_2O that these mixture association schemes offer. A conclusion that could be drawn is that more than one association scheme needs to be used, depending on the state of the system.

Similar to the pure component association schemes, to gain a perspective on the relative dominance of specific oligomers in the mixture, the predictive ability of the self-association cases were studied. In the next section, the predictive ability of these models on some of the available experimental data is discussed.

Mixture Predictions: Self-Association Case. In Figure 13, the density results that are obtained from various association schemes are shown. As one can see, almost all the schemes reported in Figure 13 capture the unusual liquid density peak that is exhibited by the aqueous HF experimental data. The % AAD values for all the association schemes are reported in Table 11.

The 1−4 and 1−2−3−4−6 association scheme predicts the mixture density best in comparison with all other schemes. The 1−2−6−8 and 1−6 association schemes overpredict the density peak in comparison with the 1−4 and 1−2−3−4−6 scheme, and underpredict when compared to the infinite association scheme. The 1−2 association scheme, which was reported with high correlative ability (based on the low θ_{ij} value), was the poorest in predicting the mixture density in comparison with other schemes. This scheme does not even show the density peak that was reported in the experimental data and was captured by all other schemes.

While the 1−2 association scheme show poor predictive ability on the mixture density predictions, it shows good agreement with the bubble point curve at 348.15 K when compared to the other association schemes. Figure 14 shows the predicted bubble point curves from various association schemes. From the plot, it can be seen that the 1−4 and 1−2−3−4−6 schemes show reasonable correlation in comparison to the 1−2−6−8, 1−6, and infinite association schemes. Also, based on the % AAD values in Table 11, the 1−2−3−4−5 and 1−2−3 schemes predict this property with fair amount accuracy in comparison. While reporting the % AAD values in Table 11, the association

Table 11. % AAD Values of Predicted Properties from Self-Association Models

scheme	density[48]	bubble point curve 348.15 K	ΔH_{vap}	C_P
1−2	*32.2451*	**1.9697**	*18.2665*	**9.8314**
1−4	**1.1160**	**4.0134**	15.4621	**8.4346**
1−6	4.7869	5.2730	**11.3595**	20.5727
1−2−3	4.0708	**4.3289**	*22.2088*	**11.6219**
1−2−6	4.6911	5.2915	**11.8743**	21.7955
1−3−6	**2.5165**	5.2536	**11.5720**	21.4848
1−2−12	*13.5876*	*9.5821*	12.2815	*35.2810*
1−2−6−8	7.2302	6.9957	**11.7926**	*28.9579*
1−2−3−4−5	**1.1415**	**4.3684**	16.2238	24.6993
1−2−3−4−6	**1.5287**	**4.2512**	*17.4794*	19.4564
1−2−3−6−9	*8.9656*	*7.7519*	**11.9166**	*31.5049*
1→9	6.7876	6.4597	**12.0059**	*29.5248*
1→12	7.3709	6.6654	**11.6231**	25.7931
∞	*10.1405*	*9.0121*	*21.3960*	**16.2081**

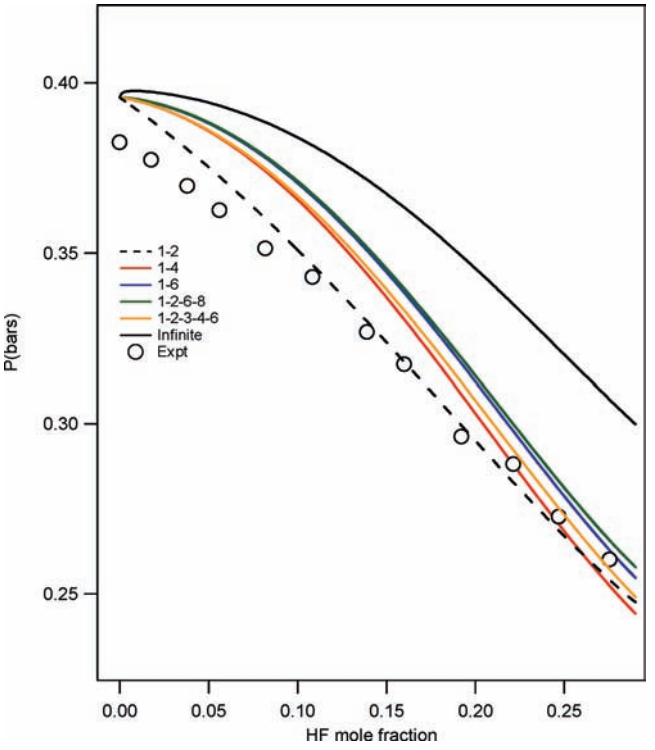

Figure 14. Aqueous HF bubble point curve at 348.15 K from various association schemes relative to the experimental data.[59]

schemes with high predictive ability are bold faced and the poor ones are italicized.

Figure 15 shows the heat of vaporization results for the mixture from various association schemes. The infinite, 1−2−3−4−6, and 1−2 schemes show poor predictions when compared to the 1−6, 1−4 and 1−2−6−8 schemes. Based on the % AAD values, all other association schemes, except for 1−2−3−4−5 and 1−2−3, show similar deviations from the experimental results.

Similar to pure HF, the mixture C_P was also evaluated numerically. The heat capacity results from various association schemes are shown in Figure 16. Here, the 1−4 and the 1−2 schemes show the best

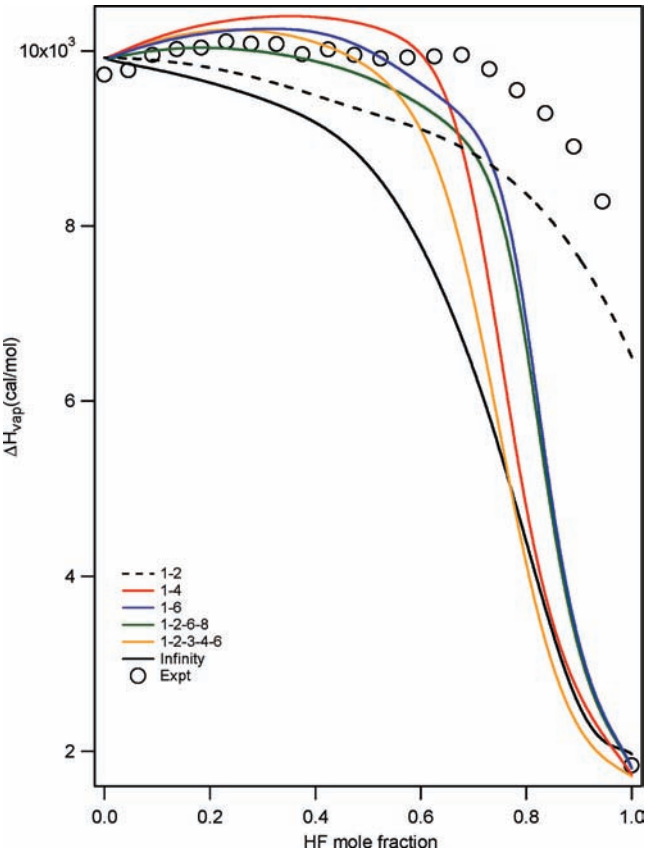

Figure 15. Aqueous HF heat of vaporization predictions from various association schemes relative to the experimental data.[60]

prediction in comparison with other association schemes. Based on the % AAD values, the 1→9, 1−2−3−6−9, 1−2−6−8, and the 1−2−3−4−5 show poor predictions when compared to the other association models. As can be seen, the inclusion of tetramers and dimers shows better predictive behavior than any other oligomers for this property. This is different from the pure HF results where the inclusion of hexamers showed improvement in the heat capacity prediction. However, it is important to understand that in this methodology the propensity of the specific association scheme should be evaluated by comparing correlative and predictive behavior in a more detailed manner, i.e., inclusion of more properties as well as association schemes. The next section will discuss the inclusion of the complex cross-association scheme in this mixture.

Formulation of the Mixture: Cross-Association Model. The chemical part of the compressibility factor is defined as the ratio of the total number of moles of all species in an associated mixture (n_T) to the total number of moles of all species that would exist without association (n_0). The Z^{ch} for a binary mixture that shows only self-association interactions was specified earlier in eq 17. Now, when the mixture is allowed to form cross-associates (i.e., association between species of HF and H_2O), the Z^{ch} is modified accordingly and can be written as

$$Z^{ch} = \frac{\sum_{i=1}^{M} n_i^{HF} + \sum_{l=1}^{L} n_l^{HF_{L1}-H_2O_{L2}} + \sum_{j=1}^{N} n_j^{H_2O}}{\sum_{i=1}^{M} i n_i^{HF} + \sum_{l=1}^{L} (L1+L2) n_l^{HF_{L1}-H_2O_{L2}} + \sum_{j=1}^{N} j n_j^{H_2O}} \quad (30)$$

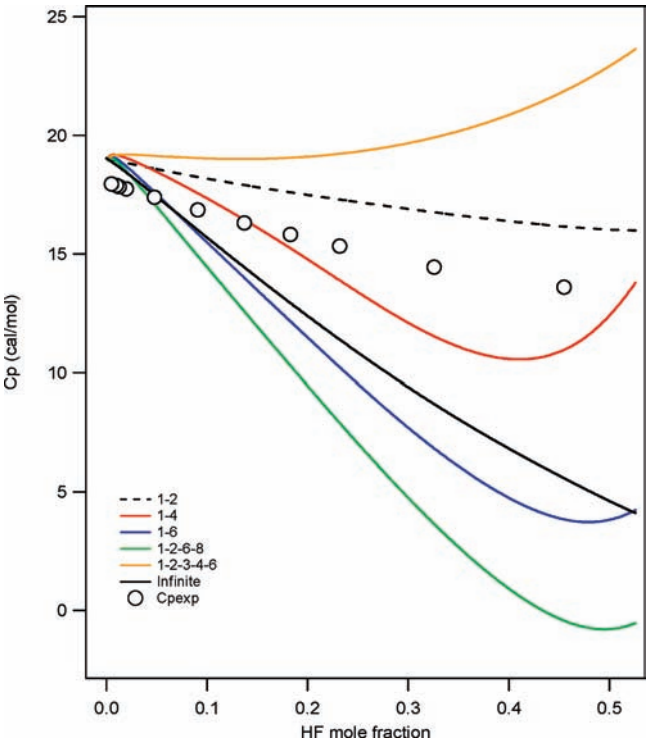

Figure 16. Aqueous HF liquid heat capacity (1 atm) predictions from various association schemes relative to the experimental data.[61]

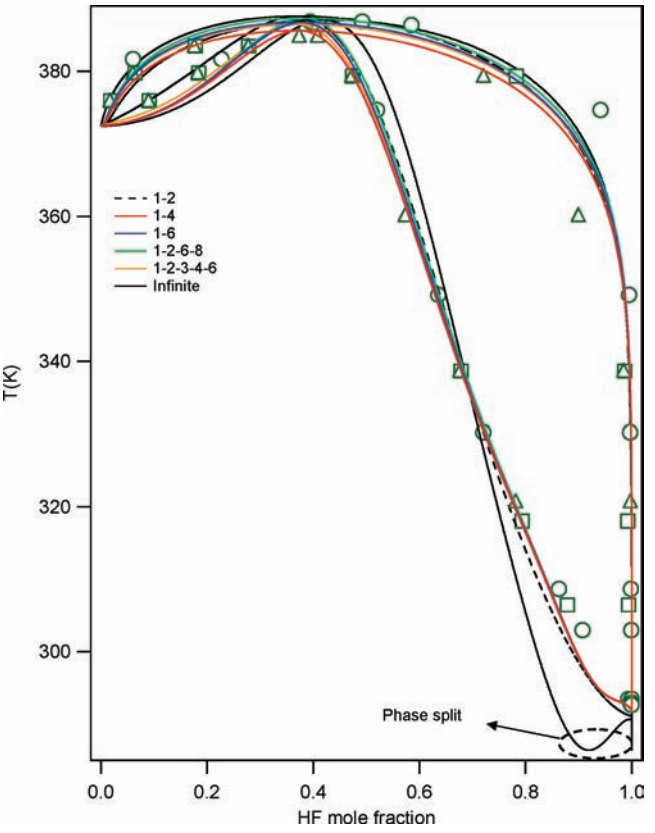

Figure 17. $T-x-y$ results for HF−H_2O system at 1 atm from various self-association schemes with a dimer cross-association. The K_{12} value for all the schemes was fixed at 0.001.

In eq 30, L signifies the number of cross-associates that are allowed to be formed by the association scheme, n_l indicates the number of moles of cross-associates in the associated mixture, and L1 and L2 are the number of HF and water molecules in the cross-associate, respectively. Similar to eq 19 that defines Z^{ch} for the case of mixture association schemes that allows only self-association, eq 30 can be modified as

$$Z^{ch} = \frac{\sum_{i=1}^{M} K_i^{HF}[Px_{HF}]^i + \sum_{j=1}^{N} K_j^{H_2O}[Px_{H_2O}]^j + \sum_{l=1}^{L} K_{L1L2}[Px_{HF}]^{L1}[Px_{H_2O}]^{L2}}{\sum_{i=1}^{M} iK_i^{HF}[Px_{HF}]^i + \sum_{j=1}^{N} jK_j^{H_2O}[Px_{H_2O}]^j + \sum_{l=1}^{L} (L1+L2)K_{L1L2}[Px_{HF}]^{L1}[Px_{H_2O}]^{L2}} \quad (31)$$

In the above equation, K_{L1L2} is the cross-association equilibrium constant, which is defined as a function of K_{12}

$$K_{L1L2} = K_{12}^{(L1+L2)-1} \quad (32)$$

where K_{12} can be considered to play the role similar to the dimerization constant in case of the pure components. So, for a cross-associate that is formed with 1 molecule of HF and 1 molecule of water, L1 = 1, L2 = 1, and $K_{L1L2} = K_{12}$. The cross-association equilibrium constant, K_{12}, can be treated as a free-parameter or as a function of self-association dimerization constants. In eq 30, if the cross-association constants are set to zero, the expression would reduce back to the self-association case described in eq 18. Once the association scheme is specified, the Z^{ch} can be calculated using the same procedure as explained for the self-association.

The fugacity coefficient is also calculated in a similar fashion as explained in the self-association case, with appropriate modifications to the ln ϕ_i^{ch} part. The derivative expression for, $N(\partial Z^{ch}/\partial n_i)_{T,v,n_j}$ is modified as

$$N\left(\frac{\partial Z^{ch}}{\partial n_i}\right)_{T,V,n_j} = \frac{\sum_{m_i=1}^{M}(1-m_iZ^{ch})m_i\left(\frac{G_i}{K_i}\right)^{m_i-1}K_{m_i} + \sum_{l=1}^{L}(1-Z^{ch}(L1+L2))L1\left(\frac{G_i}{K_i}\right)^{L1-1}\left(\frac{G_j}{K_j}\right)^{L2}K_{12}^{(L1+L2)-1}}{\sum_{m_i=1}^{M} m_i^2\left(\frac{G_i}{K_i}\right)^{m_i-1}K_{m_i} + \sum_{l=1}^{L} L1\left(\frac{G_i}{K_i}\right)^{L1-1}\left(\frac{G_j}{K_j}\right)^{L2}K_{12}^{(L1+L2)-1}} \quad (33)$$

As one can see, the fugacity coefficient expression becomes complicated as the cross-association interactions are included. Equation 33 is the derivative expression that needs to be included in eq 25, which is evaluated numerically.

In Figure 17, the correlation results of the $T-x-y$ experimental data at 1 atm for the aqueous hydrogen fluoride mixture is shown for different association schemes that include cross-association. To begin with, in all cases, the most simplistic cross-association that allows only cross-dimers, $(HF)_1-(H_2O)_1$, was included with the K_{12} value fixed in all cases. This did not have a significant effect on the binary interaction parameter value. On the other hand, the inclusion of an infinite association scheme that allows infinite self- and

dx.doi.org/10.1021/je1011955 |J. Chem. Eng. Data 2011, 56, 1506–1525

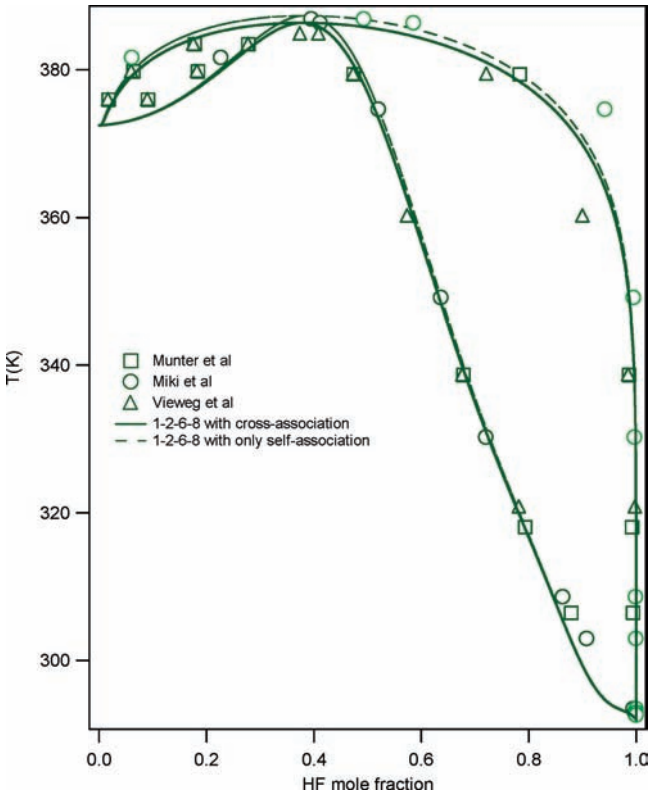

Figure 18. $T-x-y$ results for the HF−H_2O system at 1 atm from a 1−2−6−8 scheme with nine different cross-associates. The K_{12} value for all the schemes was fixed at 0.0001. Experimental data are reported as empty symbols.[53,54,58]

cross-association interactions showed some significant effects. The phase split in the concentrated HF region that was reported earlier in the infinite self-association model was more pronounced when the cross-association is included. Also, the model was reported to show double azeotrope at dilute HF conditions.

Molecular Level Distribution of Oligomers. As suggested earlier, the mixture of HF and water can potentially form a variety of cross-associates. Hence, it is prudent from a modeling standpoint to include only the cross-associates that are most likely to be present in the solution phase. Recently, a computational study was performed to study the structures and energetics of 214 different conformations of $(HF)_m(H_2O)_n$ clusters with $m + n = 2-8$.[55] These were studied using a hybrid meta density functional theory (HMDFT) study at the mPW1B95/6-31+G-(d,p) level of theory.

The primary objective of that work was to extract the cross-cluster information that can be applied in the development of a bulk-phase thermodynamic model for this particular mixture. The values of the energy and the free energy of formation for various cluster types indicate that the combinations with the same or similar number of HF and H_2O molecules are the most stable. While the energy values suggest the formation of complex networks such as cubic and cage-like structures for larger clusters, the free energy values indicate the monocyclic structures to be the most stable. Typically, a structure that forms a more complex H-bond network characterized by a lower energy does have low entropy, and this is reflected in higher free energy values.

The strength of the H-bond interactions was analyzed using multiple linear regressions. Three different regressions, based on ΔE, ΔH_0, and ΔG_{298}, indicate that the $H_2O\cdots HF$ interaction is the strongest of the four different H-bond interactions that could occur in a un-ionized cluster. The $H_2O\cdots HF$ H-bond interaction being the strongest is also consistent with the ionization of HF and formation of H_3O^+ and F^- ions, which was obtained in some clusters. Finally, an analysis was performed to provide those cross-associates that were most likely to be present at various compositions in this mixture. It is this knowledge that can be directly incorporated into a bulk-phase thermodynamic model.

The most preferred clusters, based on the Gibbs free energy values from the HMDFT study, are $(HF)_1-(H_2O)_4$, $(HF)_2-(H_2O)_4$, $(HF)_1-(H_2O)_5$, $(HF)_3-(H_2O)_3$, $(HF)_2-(H_2O)_5$, $(HF)_4-(H_2O)_2$, $(HF)_4-(H_2O)_3$, $(HF)_5-(H_2O)_1$, and $(HF)_4-(H_2O)_1$. The effect of the inclusion of these nine different clusters to the bulk-phase model was also studied.

Since the model that was developed here, at this stage, does not allow the inclusion of cross-clusters as a function of composition, all the nine clusters that were identified from the HMDFT study were included across the entire composition. However, the inclusion of these clusters also did not yield a substantial change to the binary interaction parameter values of the self-association model. The correlation results from a 1−2−6−8 association scheme with the inclusion of these nine different cross-associates that were reported in the HMDFT study are shown in Figure 18. The K_{12} value was fixed at 0.0001 for this case. Due to the computational time and the minimal changes in the binary interaction parameter values, the predictive ability of the cross-association schemes has not been explored here. At this point, the first necessary step is to modify the numerical evaluation of the fugacity coefficient for the association schemes that allows cross-interactions and to explore the parameter space for the cross-association equilibrium constant.

SUMMARY

One of the most distinguishing features of associating fluids is their highly directional and attractive molecular level interactions.[15] These interactions have profound effects on the microscopic and macroscopic properties of the fluid. The primary objective of this work was to describe a methodology for developing a robust and predictive thermodynamic model for substances showing strong association interactions. The key idea was to incorporate knowledge of how the system associates at a molecular level and to use that knowledge to correlate and predict bulk-phase thermodynamic properties. The current study was derived from the fundamental chemical theory of association proposed by Prausnitz and co-workers.[2,24,62] The methodology that is used in this work can be used to thermodynamically describe any strongly associating mixture with such substances as HCl and H_2SO_4, as well as mixtures of those substances with hydrocarbons. In this work, we have used a binary mixture containing HF and H_2O as a model to describe the methodology. The development of a thermodynamic model that allows the association interaction between two individual compounds as well as mixtures was discussed in detail.

The development of various association schemes and their effect in correlating and predicting pure component properties was discussed in this work. The phase coexistence properties of pure HF and water were correlated using models that incorporate association interactions in different forms. These association schemes were utilized to predict the properties that were not

included during the correlation stage of the model. For HF, out of the 14 different association schemes studied, 1−6, 1−2−6, 1−2−6−8 (cases 1 and 2), 1−2−3−6−9, 1→9, and 1→12 schemes were reported to perform well in correlating as well as predicting various properties over a large range of operating conditions. Also, the importance of the inclusion of a correct association scheme along with an accurate distribution of oligomers for HF was illustrated by studying the predictive ability of multiple parameter sets for the same association scheme.

The phase equilibrium properties of aqueous HF mixture were studied by including self- as well as cross-association interactions. All of the 14 different association schemes that were developed for pure HF were studied along with a 1−2 association scheme for water. The self-association schemes show good correlation with the experimental results and also exhibit reasonable predictive ability for some of the properties. The heat effects that are important during the separation stages of the operation are still not accurately predicted using these self-association models. At this point, the inclusion of the cross-association interaction provides only minimal improvement to the self-association models.

AUTHOR INFORMATION

Corresponding Author

*E-mail: bbaburao21@tntech.edu. Phone: 865-560-1442. Fax: 931-372-6352.

Notes

[†]% AAD = $100/N_{data}\sum_{i=1}^{N_{data}}(|F_{i\text{-exp}} - F_{i\text{-model}}|/F_{i\text{-exp}})$.

ACKNOWLEDGMENT

This work was supported by the American Chemical Society, Petroleum Research Fund (PRF42227-AC9) and Center for Manufacturing Research, Tennessee Technological University. We also acknowledge the Computer Aided Engineering Laboratory Personnel, Tennessee Technological University, for providing the computational facilities for this work.

REFERENCES

(1) Gupta, S.; Olson, J. D. Industrial Needs in Physical Properties. *Ind. Eng. Chem. Res.* **2003**, *42*, 6359.

(2) Heidemann, R. A.; Prausnitz, J. M. A van der Waals-type equation of state for fluids with associating molecules. *Proc. Natl. Acad. Sci. U. S. A.* **1976**, *73*, 1773–1776.

(3) Van Ness, H. C. Thermodynamics in the treatment of vapor/liquid equilibrium (VLE) data. *Pure. Appl. Chem.* **1995**, *67*, 859.

(4) Kao, C. P. C.; Paulaitis, M. E.; Sweany, G. A.; Yokozeki, M. An equation of state/chemical association model for fluorinated hydrocarbons and HF. *Fluid Phase Equilib.* **1995**, *108*, 27.

(5) Chipot, C.; Gorb, L. G.; Rivail, J. L. Proton Transfer in the Mono- and the Dihydrated Complexes of HF and HCl: An MP2/6-31+G ab Initio Study in the Self-Consistent Reaction Field Model of Solvation. *J. Phys. Chem.* **1994**, *98*, 1601.

(6) Hannachi, Y.; Silvi, B.; Bouteiller, Y. Structure and vibrational properties of water hydrogen halide complexes. *J. Chem. Phys.* **1991**, *94*, 2915.

(7) Lassonen, K; Klein, M. L. *Ab initio* Molecular Dynamics Study of Dilute Hydrofluoric Acid. *Mol. Phys.* **1996**, *88*, 135–142.

(8) Silanpaa, A. J.; Simon, C.; Klein, L. M.; Lassonen, K. Structural and Spectral Properties of Aqueous Hydrogen Fluoride Studied Using ab Initio Molecular Dynamics. *J. Phys. Chem. B* **2002**, *106*, 11315.

(9) Juwono, E.; Engineering Modeling of Hydrogen Fluoride and Water Mixture Using Statistical Associating Fluid Theory. *M.S. thesis*, State University of Buffalo, 1998.

(10) Redington, R. L. Non ideal-Associated Vapor Analysis of Hydrogen Fluoride. *J. Phys. Chem.* **1982**, *88*, 552.

(11) Giguere, P. A.; Turrel, S. The Nature of Hydrofluoric Acid. A Spectroscopic Study on the Proton Transfer Complex $H_3O^+.F^-$. *J. Am. Chem. Soc.* **1980**, *102*, 5473.

(12) Jedlovszky, P.; Vallauri, R. Computer simulations of liquid HF by a newly developed polarizable potential model. *J. Chem. Phys.* **1997**, *107*, 10166.

(13) Weast, R. C. *Handbook of Chemistry and Physics*, 68th ed.; CRC Press: Boca Raton, FL, 1988.

(14) Luck, W. A. P. Hydrogen Bonds in Liquid Water. In *The Hydrogen Bond. Recent Developments in Theory and Experiments*; Schuster, P., Zundel, G., Sandorfy, C., Ed.; North-Holland Publishing Co: Amsterdam, 1976; p 1369.

(15) Walsh, J. M.; Guedes, H. J. R.; Gubbins, K. E. Physical theory for fluids of small associating molecules. *J. Phys. Chem.* **1992**, *96*, 10995.

(16) Baburao, B.; Visco, D. P. Isothermal compressibility maxima of hydrogen fluoride in the supercritical and superheated vapor regions. *J. Phys. Chem. B* **2006**, *110*, 26204.

(17) Simons, J. H. *Fluorine Chem.* **1950**, *1*, 225.

(18) Long, R. W.; Hildebrand, J. H.; Morrell, W. E. The Polymerization of Gaseous Hydrogen Fluoride and Deuterium Fluorides. *J. Am. Chem. Soc.* **1943**, *65*, 182.

(19) Briegleb, G.; Strohmeier, W. Association of hydrogen fluoride in the gaseous state. II. *Z.Elektrochem.* **1953**, *57*, 668.

(20) Twu, C. H.; Coon, J. E.; Cunningham, J. R. An Equation of State for Hydrogen Fluoride. *Fluid Phase Equilib.* **1993**, *37*, 158–160.

(21) Visco, D. P.; Kofke, D. A. Improved Thermodynamic Equation of State for Hydrogen Fluoride. *Ind. Eng. Chem. Res.* **1999**, *38*, 4125–4129.

(22) Galindo, A.; Whitehead, P. J.; Jackson, G.; Burgess, N. A. Predicting the Phase Equilibria of Mixtures of Hydrogen Fluoride with Water, Difluoromethane (HFC-32), and 1,1,1,2- Tetrafluoroethane (HFC-134a) Using a simplified SAFT approach. *J. Phys. Chem. B* **1997**, *101*, 2082–2091.

(23) Baburao, B. Thermodynamic modeling of aqueous hydrogen fluoride mixtures. *Dissertation*, Tennessee Technological University, 2007

(24) Whiting, W. B.; Prausnitz, J. M. A new equation of state for fluid water based on hard-sphere perturbation theory and dimerization equilibria. *International Conference on the Properties of Steam*, Munich, Germany, September, 1979.

(25) Lencka, M.; Anderko, A. Modeling phase equilibria in mixtures containing hydrogen fluoride and halocarbons. *AIChE J.* **1993**, *39*, 533.

(26) Baburao, B.; Visco, D. P. VLE/VLLE/LLE Predictions for Hydrogen Fluoride Mixtures Using an Improved Thermodynamic Equation of State. *Ind. Eng. Chem. Res.* **2002**, *41*, 4863.

(27) Wooley, H. W. The Representation of Gas Properties in Terms of Molecular Clusters. *J. Chem. Phys.* **1953**, *21*, 236.

(28) Anderko, A. Phase equilibria in aqueous systems from an equation of state based on the chemical approach. *Fluid Phase Equilib.* **1991**, *65*, 89.

(29) Baburao, B.; Visco, D. P. Association based equation of state for substances forming monomers, dimers and trimers. *Fluid Phase Equilib.* **2008**, *265*, 7–11.

(30) Peng, D.-Y.; Robinson, D. B. A New Two-Constant Equation of State. *Ind. Eng. Chem. Fundam.* **1976**, *15*, 59.

(31) Anderko, A. Extension of the AEOS model to systems containing any number of associating and inert components. *Fluid Phase Equilib.* **1989**, *50*, 21.

(32) Luckhaus, D.; Quack, M.; Schmitt, U.; Suhm, M. A. On FTIR Spectroscopy in Asynchronously Pulsed Supersonic Free Jet Expansions and on the Interpretation of Stretching Spectra of HF Clusters. *Berichte der Bunsengesellschaft für physikalische Chemie* **1995**, *99*, 457–468.

(33) Galindo, A.; Burton, S. J; Jackson, G.; Visco, D. P.; Kofke, D. A. Improved Models for the Phase Behaviour of Hydrogen Fluoride: Chain and Ring Aggregates in the SAFT Approach and the AEOS Model. *Mol. Phys.* **2002**, *100*, 2241–2259.

(34) Zhang, C.; Freeman, D. L.; Doll, J. D. Monte Carlo Studies of Hydrogen Fluoride Clusters: Cluster Size Distributions in Hydrogen Fluoride Vapor. *J. Chem. Phys.* **1989**, *91*, 2489.

(35) Reklaitis, G. V.; Ravindran, A.; Ragsdell, K. M. *Engineering optimization methods and applications*; Wiley-Interscience: New York, 1983.

(36) Nemethy, G.; Scheraga, H. A. Structure of Water and Hydrophobic Bonding in Proteins. I. A Model for the Thermodynamic Properties of Liquid Water. *J. Chem. Phys.* **1962**, *36*, 3382.

(37) Davis, C. M., Jr.; Litovitz, T. A. Two-State Theory of the Structure of Water. *J. Chem. Phys.* **1965**, *42*, 2563.

(38) Jhon, M. S.; Grosh, J.; Ree, T.; Eyring, H. Significant-Structure Theory Applied to Water and Heavy Water. *J. Chem. Phys.* **1966**, *44*, 1465.

(39) Owicki, J. C.; Shipman, L. L.; Scheraga, H. A. Structure, energetics, and dynamics of small water clusters. *J. Phys. Chem.* **1975**, *79*, 1794.

(40) Visco, D. P.; Kofke, D. A.; Singh, R. Thermal Properties of Hydrogen Fluoride from an EOS + Association Model. *AIChE J.* **1997**, *43*, 2318–2384.

(41) Atkins, P. W. *Physical Chemistry*, 2nd ed.; W. H. Freeman and Co.: San Francisco, 1982.

(42) Walas, S. M. *Phase equilibria in chemical engineering*; Buttterworth Publishers: London, 1985.

(43) Frank, E. U.; Meyer, F. Specific heat and association in the gas phase at low pressure. *Z. Elektrochem.* **1959**, *63*, 571.

(44) Hu, J. H.; White, D.; Johnson, H. L. The Heat capacity, Heat of Fusion and Heat of Vaporization of Hydrogen Fluoride. *J. Am. Chem. Soc.* **1953**, *75*, 1232.

(45) Franck, E. U.; Spalthoff, W. Hydrogen Fluoride I. Specific Heat, Vapor pressure and Density up to 300 °C and 300 atm. *Z.Elektrochem.* **1957**, *61*, 348.

(46) Franck, E. U.; Wiegand, G.; Gerhardt, R. The Density of Hydrogen Fluoride at high Pressures to 979 K and 200 MPa. *J. Supercrit. Fluids* **1999**, *15*, 127.

(47) Karger, N.; Tarassov, N.; Ludemann, H. Density of Liquid Hydrogen Fluoride between 258 and 373 K at Pressures up to 200 MPa. *J. Chem. Eng. Data* **1998**, *43*, 931.

(48) Anderko, A. Modeling phase equilibria using an equation of state incorporating association. *Fluid Phase Equilib.* **1992**, *75*, 89.

(49) Prausnitz, J. M.; Tavares, F. W. Thermodynamics of Fluid-Phase Equilibria for Standard. Chemical Engineering Operations. *AIChE J.* **2004**, *50*, 739.

(50) Wei, Y. S.; Sadus, R. J. Equations of state for the calculation of fluid-phase equilibria. *AIChE J.* **2000**, *46*, 169.

(51) Prausnitz, J. M.; Lichtenthaler, R. N.; Gomez de Azevedo, E. *Molecular Thermodynamics of Fluid-Phase Equilibria*, 3rd ed.; Prentice Hall: Englewood Cliffs, NJ, 1999.

(52) Smith, C.; Visco, D. P. Evaluating the Thermodynamic Consistency of Experimental Data for HF + H_2O at 101.325 kPa. *J. Chem. Eng. Data* **2004**, *49*, 306–310.

(53) Vieweg, R. Ein Enthalpie-Konzentrations-Digramm des Systems Fluorowasserstoff-Wasser. *Chem. Technol. (Berlin)* **1963**, *15*, 734.

(54) Miki, N.; Maeno, M.; Maruhasi, K.; Ohmi, T. Vapor-Liquid Equilibrium of the Binary System HF-H_2O Extending to Extremely Anhydrous Hydrogen Fluoride. *J. Electrochem. Soc.* **1990**, *137*, 787.

(55) Baburao, B.; Visco, D. P.; Albu, T. V. Association Patterns in $(HF)_m(H_2O)_n$ $(m + n = 2-8)$ Clusters. *J. Phys. Chem. A* **2007**, *111*, 7940–7956.

(56) Van Wylen, G. J.; Sonntag, R. E. *Fundamentals of Classical Thermodynamics*, 2nd ed.; John Wiley & Sons, Inc.: New York, 1973.

(57) Fredenhagen, K. Physikalisch-chemische Messungen am Fluorwasserstoff. II. *Z. Anorg. Allg. Chem.* **1934**, *218*, 161.

(58) Munter, P. A.; Aepli, O. T.; Kossatz, R. A. Hydrofluoric Acid-Water and Hydrofluoric Acid-Hydrofluosilicic Acid-Water. *J. Ind. Eng. Chem.* **1947**, *39*, 427.

(59) Brosheer, J. C.; Lenfesty, F. A.; Elmore, K. L. Vapor Pressure of Hydrofluoric Acid Solutions. *J. Ind. Eng. Chem.* **1947**, *39*, 423.

(60) Tyner, M. Enthalpy concentration diagram for hydrogen fluoride water system at one atmosphere. *Chem. Eng. Prog.* **1949**, *45* (No. 1), 49.

(61) Thorvaldson, T.; Bailey, E. C. The heat capacity of aqueous solutions of hydrofluoric acid. *Can. J. Res.* **1946**, *24B*, 51.

(62) Anderko, A.; Prausnitz, J. M. On the relationship between the equilibrium constants of consecutive association reactions. *Fluid Phase Equilib.* **1994**, *95*, 59–71.